Comparative study of modern heuristic algorithms for global maximum power point tracking in photovoltaic systems under partial shading conditions

Kangshi Wang[1,2], Jieming Ma[1]*, Ka Lok Man[1], Kaizhu Huang[3] and Xiaowei Huang[2]

[1]School of Advanced Technology, Xi'an Jiaotong-Liverpool University (XJTLU), Suzhou, China, [2]Department of Computer Science, University of Liverpool, Liverpool, United Kingdom, [3]Data Science Research Center, Duke Kunshan University, Suzhou, China

Under partial shading conditions (PSCs), photovoltaic (PV) generation systems exhibit multiple local and a single global maximum power point. Consequently, global maximum power point tracking (GMPPT) is required to improve the performance of PV systems in such scenarios. This paper comparatively studies and evaluates the tracking performance of modern heuristic-optimization-based GMPPT techniques. Monte Carlo method is used to statistically analyze different methods. Simulation and experimental results indicate that many of the algorithms have difficulties in balancing the explorative and exploitative searching behaviors. Therefore, we propose a variable vortex search (VVS), which is capable of improving the performance of GMPPT by using a variable step size and deterministic starting points. This paper will aid researchers and practical engineers to gain a thorough understanding on how to use modern heuristic algorithms for maximum power out of PV systems. Furthermore, it offers a comprehensive guidance on how to perform efficiently GMPPT in the PV systems under PSCs.

KEYWORDS

maximum power point tracking (MPPT), partial shading condition (PSC), heuristic optimization, solar PV (SPV) systems., vortex search (VS.) algorithm, global maximum power point (GMPP) tracking

1 Introduction

As a renewable, clean, and convenient energy source, photovoltaic (PV) is a promising technology that is doubling in size every 1–2 years globally (Xiao et al., 2016; Danandeh et al., 2018; Kabir et al., 2018). Since the output power of a PV system varies with the atmospheric conditions (e.g., temperature and solar irradiance), the maximum power point tracking (MPPT) technology is necessitated for extracting the maximum power available in PV systems (Zhou et al., 2021).

When part of a PV string is shaded by fallen leaves, clouds, or building shadows, etc., these shaded parts act as loads and absorb energy (Bana and Saini, 2017; Atems and Hotaling, 2018). The non-uniform solar irradiance will lead to hot spots and cause the entire PV string to lose efficiency. Bypass diodes are introduced to shift the redundant current and prevent the hot spots (Seyedmahmoudian et al., 2016; Li G et al., 2018). Under partial shading conditions (PSCs), multiple peaks are exhibited in the power-voltage (P-V) curve, which bring challenges to the optimization of the power conversion. Among these peaks, there exist several local maximum power points (LMPPs) and a single global maximum power point (GMPP) (Rezk et al., 2017). Traditional MPPT approaches, such as perturbation and observation (P&O) (Kavya and Jayalalitha, 2021), incremental conductance (InC), short circuit current (SCC) technique (Reisi et al., 2013), constant voltage (CV) technique, and reference voltage based track optimizer (Deboucha et al., 2021; Li et al., 2022), track the GMPP using a defined step length and are based on a single peak P-V curve. These methods can find the MPP quickly under the uniform irradiation conditions (UICs) because of their excellent local search ability (Kjær, 2012; Li H et al., 2018; Ahmad et al., 2019), but they may find the LMPP instead of the GMPP under the PSCs due to the lack of global optimization ability.

The heuristic optimization algorithms, which can normally obtain better exploratory capacity, have been used to address the global maximum power point tracking (GMPPT) problems in the last decade or so (Motahhir et al., 2020; Yang et al., 2020; Díaz Martínez et al., 2021). These algorithms include salp swarm optimization algorithm (Mirza et al., 2021), particle swarm optimization (PSO) (Khare and Rangnekar, 2013; Shi et al., 2015; Soufi et al., 2017; Li H et al., 2018; Eltamaly et al., 2020), shuffled frog leaping algorithm (SFLA) (Eusuff et al., 2006; Neri and Cotta, 2012; Sridhar et al., 2017; Mao et al., 2018), artificial bee colony algorithm (ABCA) (Fathy, 2015; Soufyane Benyoucef et al., 2015; Sundareswaran et al., 2015a; Jadon et al., 2017; Pilakkat and Kanthalakshmi, 2019; Pilakkat and Kanthalakshmi, 2020), cuckoo search (CS) (Yang and Deb, 2013; Ahmed and Salam, 2014; Mareli and Twala, 2018; Mosaad et al., 2019; Mosaad et al., 2019; Eltamaly, 2021), firefly algorithm (FA) (Lones, 2014; Teshome et al., 2016; Wang and Liu, 2019), teaching learning based optimization (TLBO) (Rao et al., 2012; Chao and Wu, 2016; Rezk and Fathy, 2017), water cycle algorithm (WCA) (Eskandar et al., 2012; Sarvi et al., 2014), flower pollination optimization (FPO) (Yang, 2012; Diab and Rezk, 2017; Samy et al., 2019; Yousri et al., 2019; Sundararaj et al., 2020), vortex search (VS) (Doğan and Ölmez, 2015; Ali et al., 2018), Jaya algorithm (Jaya) (Padmanaban et al., 2019; Rao, 2016; Rao and Saroj, 2017; Huang et al., 2017b; Huang et al., 2017a), monarch butterfly optimization (MBO) (Wang et al., 2019), satin bowerbird

optimization (SBO) (Moosavi and Bardsiri, 2017), yellow saddle goatfish algorithm (YSGA) (Zaldivar et al., 2018), artificial ecosystem-based optimization (AEO) (Zhao et al., 2019), electric fish optimization (EFO) (Yilmaz and Sen, 2019), harris hawks optimization (HHO) (Heidari et al., 2019; Mansoor et al., 2020), and sparrow search algorithm (SSA) (Xue and Shen, 2020). Inspired by the biological performance or the physical phenomenon, most of these algorithms can find the GMPP after a few iterations. To further improve the tracking efficiency, Sundareswaran et al. (2015a) proposed a P&O algorithm assisted through a colony of foraging ants (CFA) method. The CFA technique successfully blends ant-colony-based global search in the early stages of tracking with the standard P&O method in the latter stages for exploitative search. The genetic and cuckoo search algorithms are used to increase the exploitative search ability of P&O in (Ahmed et al., 2021). In Lian et al. (2014), implemented the P&O for the first round and the PSO for the second round of search. The P&O method reduces the search space of the PSO. However, the inherent demerits of heuristic optimization methods still cannot be avoided. The initial positions of candidate solutions seriously affect the tracking performance of GMPPT (Shams et al., 2020). Another demerit is that multiple parameters are required in many heuristic methods. Tuning of parameters is a time consuming process and decreases the agileness of implementation (Koad et al., 2016). Besides, many heuristic optimization methods choose the search behaviors by different parameter settings, thus suffering from the problem of parameter dependence (Koad et al., 2016). As a generic remark, there are already a good number of publications on this issue (Eltamaly et al., 2018), categorizing and summarizing existing MPPT approaches is critical for future study. In addition, it can be noticed that although heuristic algorithms have been widely used for global maximum power point tracking (GMPPT) (Mao et al., 2020), there lacks qualitative and quantitative study work on these algorithms.

Motivated by the above situation, twelve heuristic-optimization-based GMPPT methods are comparatively studied in this paper. Both software simulations and hardware experiments are conducted for statistical evaluation. Most of these methods lack an efficient mechanism to balance the explorative and exploitative searching behaviors. Furthermore, we develop a novel variable-vortex-search (VVS) based GMPPT method. The starting points of the algorithm are determined by a pre-search strategy so that the search space is reduced. Then the search behavior of the VVS is modeled as a vortex pattern by using a variable step size and mountain-like tracking scheme according to the Gaussian distribution. In the test, the proposed method is compared with eleven heuristic- optimization-based GMPPT methods in terms of tracking routines, accumulated energy, accuracy and tracking efficiency.

FIGURE 1
A typical PV string and the I-V and P-V characteristics of a 3 PV modules string under different shading conditions.

FIGURE 2
Classification of the modern heuristic algorithms.

FIGURE 3
The search process of the VVS under the PSC (G1 = 1000 W/m^2, G2 = G3 = 800 W/m^2, G4 = 600 W/m^2): **(A)** Pre-search; **(B)** Determination of the initial points; **(C)** An illustrative sketch of the VVS optimization.
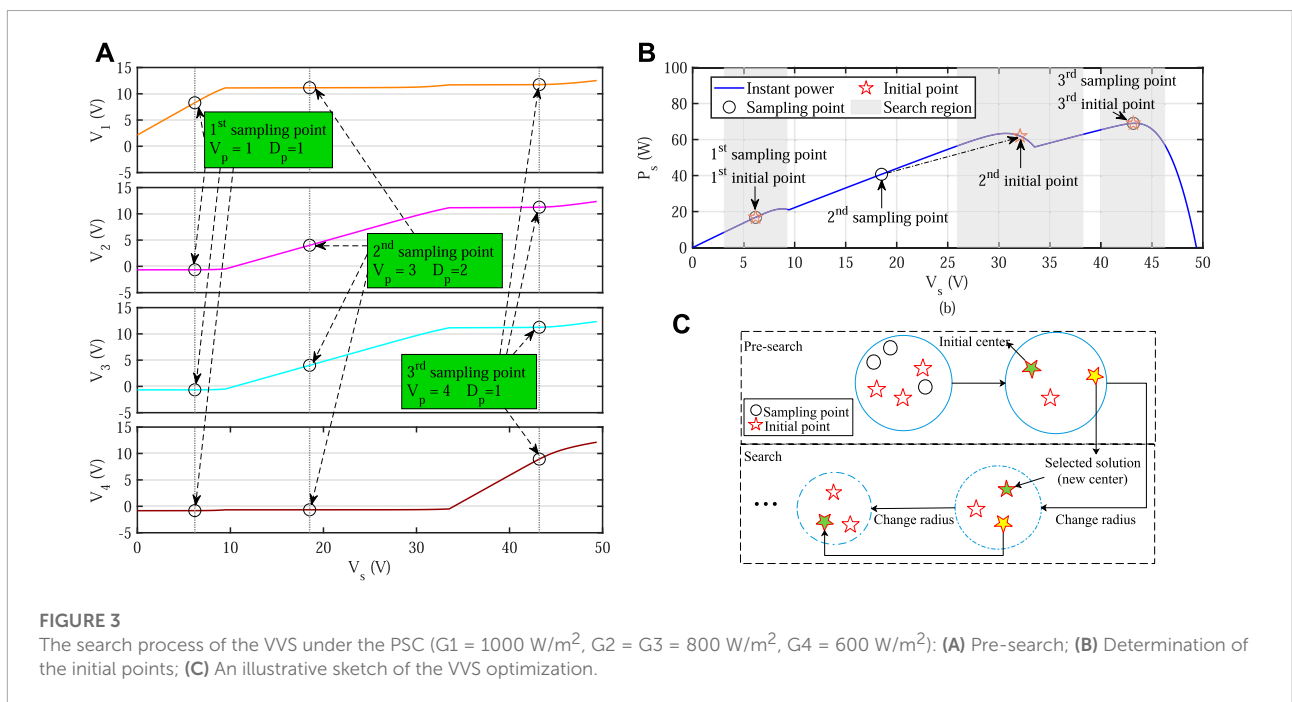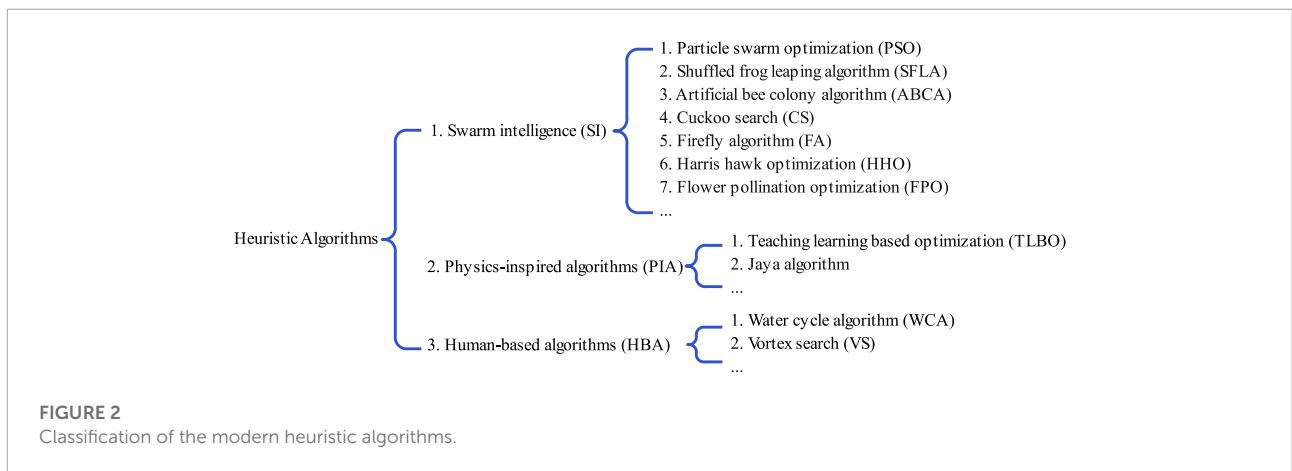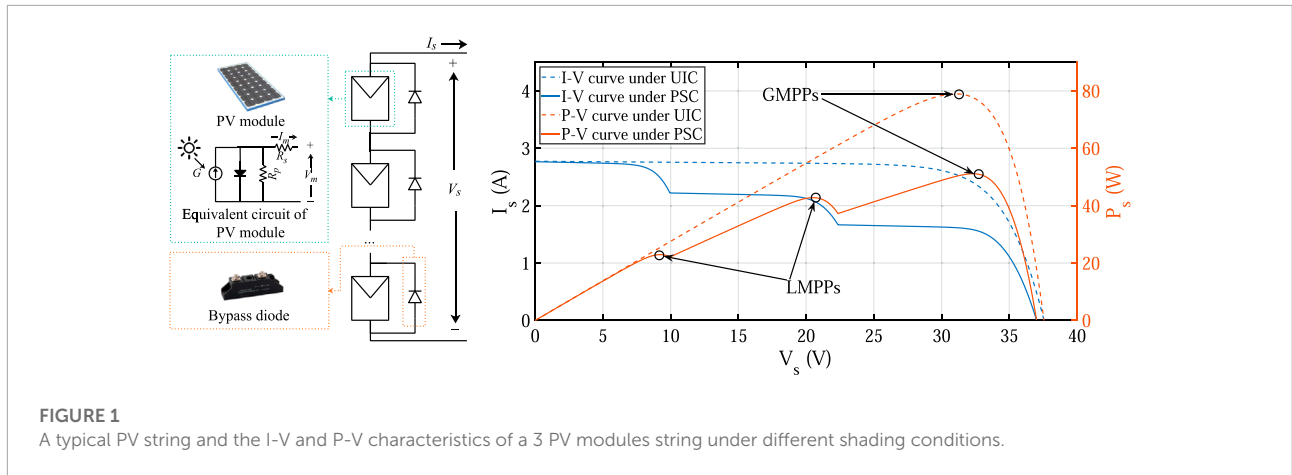
TABLE 1 Specifications of the Sanyo HIT-N225A01 module, Kyocera KC175GT module and Jinghai JH-10 module.

Parameter	HIT-N225A01	KC175GT	JH-10
Maximum Power P_{mpp}	215.46 W	175.11 W	9.44 W
Open Circuit Voltage V_{oc}	51.60 V	29.20 V	10.24 V
Short Circuit Current I_{sc}	5.61 A	8.09 A	1.33 A
Voltage at P_{mpp}	42.00 V	23.60 V	8.50 V
Current at P_{mpp}	5.13 A	7.42 A	1.11 A
Cells per Module	72	48	20

TABLE 2 Partial shading patterns for the step test.

Shading pattern	Solar irradiance (W/m^2)			GMPP (W)
	M1	M2	M3	
1	500	200	100	11.52
2	800	400	100	20.59
3	1100	900	300	49.31

The main contributions of this paper are highlighted as follows:

1. This paper statistically investigates modern heuristic optimization methods for GMPPT in PV systems under PSCs.
2. The challenges of heuristic-optimization-based GMPPT techniques, especially the exploitative and explorative search capabilities, have been analyzed through a comprehensive study.
3. A novel VVS-based GMPPT, which is capable of balancing the exploitative and explorative search capabilities, is proposed.
4. Experimental comparisons of different heuristic-optimization-based GMPPT techniques in terms of the tracking routines, accumulated energy, and tracking efficiency are presented.

The following sections are organized as follows: the characteristics of the PV strings are discussed in **Section 2**. A comprehensive study of existing heuristic-optimization-based GMPPT methods, followed by the proposed variable-vortex-search (VVS) based GMPPT method, is presented in **Section 3**. The simulation and experimental findings are discussed in **Section 4**. **Section 5** concludes this paper.

2 Electrical characteristics of the PV strings under partial shading conditions

When bypass diodes are considered, the output I-V relations of a PV module could be expressed as an extension to its single-diode model, which can be written as **Eq. 1**

(Bouraiou et al., 2015; Ram et al., 2018).

$$I_s = I_{pv} - I_{sat}\left[exp\left(q\frac{V_s + I_s R_s}{N_s k T \eta}\right) - 1\right] - \frac{V_s + I_s R_s}{R_p} + I_{bp} \quad (1)$$

where I_{pv} is the photo-generated current, I_{sat} is the reverse bias saturation current of the diode, N_s is the number of PV cells connected in series on the specified PV module, q is the electron charge constant ($1.60217 \times 10^{-19} C$), k is the Boltzmann constant ($1.38065 \times 10^{-23} J/K$), T is the temperature of the PN junction, η is the diode ideality constant, R_s is the series resistance, and R_p is the shunt resistance. The PV modules which are subject to low solar irradiance will produce less current than the unshaded modules at the same temperature. Therefore, the mismatch losses are caused. This kind of mismatch losses can be avoided by the bypass diodes. The current flow *via* the bypass diode may be calculated using **Eq. 2**.

$$I_{bp} = I_{sat, bp}\left[exp\left(q\frac{V_s}{k T \eta}\right) - 1\right] \quad (2)$$

where $I_{sat, bp}$ is the reverse bias saturation current of the bypass diode.

The structure of a PV string is shown in **Figure 1**. According to Kirchhoff's law, the system of nonlinear equations for a PV string can be expressed by **Eq. 3** (Ma et al., 2022).

$$V_1 + V_2 + \cdots + V_N - V_s = 0$$
$$I_1(V_1) - I_2(V_2) = 0$$
$$I_1(V_1) - I_3(V_3) = 0$$
$$\cdots$$
$$I_1(V_1) - I_N(V_N) = 0 \quad (3)$$

In **Figure 1**, the I-V and P-V characteristics of a PV string under uniform irradiance conditions (UICs) and PSCs are displayed. It can be seen that the PV system performs staircase-like I-V curves while its P-V characteristics exhibit multiple peaks under PSCs. Under PSCs, traditional MPPT approaches such as the P&O and InC will be locked in the LMPPs, resulting in energy losses. As a result, it is critical to investigate MPPT algorithms capable of handling PSCs.**Figure 2**

3 Heuristic-optimization-based global maximum power point tracking

Many researchers tried to tackle the GMPPT under PSCs *via* heuristic optimization techniques. Generally, these techniques can be roughly categorized into three major classes: swarm intelligence (SI), physics-inspired algorithms (PIA), and human-based algorithms (HBA) (Gogna and Tayal, 2013). The SI techniques mimic creatures in nature. The physical laws inspire the PIA approaches. Similarly, HBA are developed based on human traits and behaviours. The classification of the modern heuristic algorithms reviewed in this paper is summarized in.

TABLE 3 Average test results of KC175GT, HIT-N224A01, and JH-10 PV string.

Module	Topology	Metric	3S				5S				7S			
			Peff	Tmin	Vmae	Vrmse	Peff	Tmin	Vmae	Vrmse	Peff	Tmin	Vmae	Vrmse
KC175GT		VVS	0.7292	0.3615	1.3840	3.0212	0.7059	0.2862	1.8511	5.7872	0.6860	0.4081	4.3976	10.3599
		VS	0.7634	0.4401	4.6103	10.4963	0.7611	0.4871	11.2462	20.0649	0.7403	0.5835	19.8341	31.7224
		PSO	0.7103	0.4518	6.1450	12.3102	0.6920	0.4423	8.9100	16.5568	0.6709	0.4131	13.0637	22.2617
		WCA	0.7264	0.4621	4.8553	11.3281	0.7416	0.4680	7.8873	16.9926	0.7522	0.4629	11.4599	23.2406
		TLBO	0.6658	0.4930	6.3234	13.1033	0.6884	0.4984	9.3941	18.7740	0.7002	0.4971	12.6361	24.2546
		SFLA	0.6895	0.2908	7.7168	11.8670	0.7044	0.2885	11.8068	17.2802	0.7082	0.2857	15.8014	22.8061
		Jaya	0.6103	0.4665	3.5196	8.8244	0.6387	0.4870	5.9259	13.7647	0.6538	0.4842	8.6133	18.2396
		HHO	0.5458	0.3972	6.0773	11.1508	0.5605	0.4028	10.0360	17.1084	0.5712	0.4100	14.2941	23.2507
		FPO	0.5584	0.4130	6.2162	11.4067	0.5745	0.4176	9.6258	16.6878	0.5825	0.4175	14.0152	23.4637
		FAO	0.5491	0.3129	8.2052	13.0248	0.5523	0.3142	13.4905	20.4791	0.5572	0.3141	18.7219	27.3415
		CS	0.6360	0.3544	5.2698	10.3245	0.6541	0.3729	8.3399	15.6225	0.6650	0.3776	11.1172	19.8944
		ABCA	0.5941	0.4042	6.1470	10.6913	0.6106	0.4058	9.3351	15.1271	0.6150	0.3971	12.4069	19.5934
HIT-N224A01		VVS	0.7306	0.3686	4.8536	13.9241	0.6926	0.2960	4.0407	11.1899	0.6887	0.3739	9.3400	25.7758
		VS	0.7612	0.4457	10.6653	24.6511	0.7504	0.4946	19.7546	34.6505	0.7440	0.5901	35.3014	56.9929
		PSO	0.6889	0.4407	13.9246	25.3703	0.6566	0.4114	19.3904	31.8556	0.6563	0.3622	27.1686	44.2136
		WCA	0.7247	0.4593	10.8533	24.5217	0.7354	0.4711	13.4298	28.4810	0.7566	0.4660	20.5600	42.4356
		TLBO	0.6627	0.4964	12.3596	24.9131	0.6816	0.5051	16.6975	32.6977	0.7020	0.5001	23.7781	46.1194
		SFLA	0.6857	0.2923	13.0906	19.7798	0.7016	0.7016	20.8352	30.1560	0.7095	0.2869	28.2671	41.5631
		Jaya	0.6085	0.4705	8.8459	21.6116	0.6282	0.4840	10.2240	21.9412	0.6552	0.4877	16.0805	34.5364
		HHO	0.5446	0.3930	12.1187	22.4600	0.5529	0.4084	17.4460	28.7437	0.5731	0.4113	26.1473	43.2926
		FPO	0.5563	0.4105	12.3833	22.9662	0.5633	0.4197	17.5990	29.4070	0.5851	0.4172	26.1580	43.8719
		FAO	0.5441	0.3074	16.4314	26.3940	0.5453	0.3118	23.5197	34.6037	0.5567	0.3108	34.0223	50.1028
		CS	0.6323	0.3533	10.6249	20.9019	0.6462	0.3737	14.7389	26.0812	0.6684	0.3789	21.0630	38.2667
		ABCA	0.5858	0.4034	10.5133	17.7175	0.6071	0.4007	16.4042	25.6902	0.6144	0.4007	23.4156	37.6711
JH-10		VVS	0.7022	0.3573	0.3146	0.6500	0.7105	0.2717	0.6609	1.9664	0.6810	0.3714	8.7619	23.1243
		VS	0.7583	0.4224	1.6663	4.0287	0.7739	0.4612	4.9038	8.7356	0.7381	0.5899	36.7684	60.7949
		PSO	0.7082	0.4350	1.8195	4.1489	0.7405	0.4457	3.0214	6.3342	0.6523	0.3730	26.9949	45.3282
		WCA	0.7317	0.4446	1.7578	4.3908	0.7583	0.4408	3.3465	7.2814	0.7515	0.4661	21.0651	45.2764
		TLBO	0.6710	0.4808	2.2635	4.9251	0.7016	0.4847	3.9916	7.9093	0.6957	0.5107	22.5156	44.6761
		SFLA	0.6888	0.2795	3.0516	4.5043	0.7089	0.2843	5.0481	7.4017	0.7042	0.2833	27.8225	41.2903
		Jaya	0.6140	0.4523	1.3104	3.3730	0.6568	0.4581	2.5404	5.8160	0.6525	0.4888	17.1189	38.5659
		HHO	0.5446	0.4000	2.2432	4.1329	0.5714	0.3926	4.3467	7.4492	0.5675	0.4147	25.7862	44.5477
		FPO	0.5535	0.4034	2.2807	4.2317	0.5844	0.4089	4.2692	7.4822	0.5812	0.4219	25.7801	44.6542
		FAO	0.5564	0.3202	3.1875	5.1207	0.5674	0.3129	5.6546	8.6538	0.5522	0.3161	34.6621	52.7115
		CS	0.6362	0.3517	1.9378	3.7798	0.6661	0.3651	3.5082	6.5930	0.6612	0.3884	21.1605	39.7959
		ABCA	0.5915	0.4000	2.3305	3.8253	0.6146	0.3958	4.1620	6.7120	0.6100	0.4023	22.5883	36.5741

3.1 Swarm intelligence techniques

3.1.1 Particle swarm optimization

PSO is inspired by birds' interactions (Eberhart and Kennedy, 1995). The population V composed of m particles is randomly initialized in the feasible space at the beginning of the algorithm. The position of each particle V_i represents a voltage set-point. In each iteration, the particle updates its speed which is the change in voltage according to the individual best solution p_i which is found by itself and the global best solution p_g according to Eqs 4, 5.

$$v_i^{t+1} = w v_i^t + n_1 \mathcal{R}_{0,1} \left(p_i - Z_i^t \right) + n_2 \mathcal{R}_{0,1} \left(p_g - Z_i^t \right) \quad (4)$$

$$V_i^{t+1} = V_i^t + v_i^{t+1} \quad (5)$$

where v_i^{t+1} represents the ith particle's speed in the $t+1$ iteration, w is the inertia weight, n_1 and n_2 are the learning constants.

There are only three parameters in PSO, making it easy to implement (Khare and Rangnekar, 2013). However, it has a proclivity to become trapped in LMPPs. To increase the tracking accuracy of PSO-based GMPPT, Shi et al. (2015) proposed a dormant PSO (DPSO) to exploratively search the area of the GMPP, and then the conventional InC algorithm will be used to track the maximum output power of PV strings. Li H et al. (2018) pointed out that PSO is very sensitive to the initial values. They proposed an overall distribution PSO (OD-PSO) to shrink the search region. In OD-PSO, the PSO algorithm is improved so that each particle tends to be within a Cauchy distribution range with the global best position, rather than the global best position itself. In Eltamaly et al. (2020), a fast adaptive PSO strategy for PV global peak tracker under dynamic PSCs are presented. The problem of a long convergence time was handled by changing the duty ratio of the dc-dc boost converter's initial values to the possible MPP locations. By boosting the ability of exploitative search, this improvement decreases the convergence time and avoids the early convergence of the original PSO.

3.1.2 Shuffled frog leaping algorithm

SFLA mimics the behaviour of a group of frogs as they look for the spot with the most accessible food. In the SFLA, the position of each frog represents a feasible solution. There are several rocks in the pond where the frogs are located. In each generation, the frogs will be allocated to the rocks. Only the frog with the worst position on the rock will jump. The frog will first jump towards the optimal position on the same rock. If the new position is worse than the previous one, it will move to the global optimal. Otherwise, it will jump randomly in the feasible area (Eusuff et al., 2006).

In the SFLA, the frogs are divided into sub-populations cyclically. A certain number of evaluations are permitted for a sub-population of m frogs. In each evaluation, the best frog is P_b,

and the worst frog is P_w. The distance of the worst frog trying to move is expressed in Eq. 6.

$$P_w^{t+1} = P_w^t + \mathcal{R}_{0,1} \times \left(P_b^t - P_w^t \right) \quad (6)$$

If Eq. 6 can produce a better solution, the frog's position will be updated. SFLA is unique in that it generates new solutions through the grouping operators and mimetic fusion (Neri and Cotta, 2012). This evolution mechanism selects the best and the worst solutions of sub-populations and realizes independent evolution.

A benchmark test in Sridhar et al. (2017) demonstrates that SFLA performs better than P&O, PSO, and differential evolution (DE) in power extracted, convergence, conversion efficiency, dynamic response, and oscillations. Particularly, the SFLA introduces the grouping concept to the optimization algorithm, and the direction of SFLA's particle is not affected by the best or worst individual but by a group of frogs on a rock. The grouping concept was combined with PSO to make an application of grid-connected modular PV converter system in Mao et al. (2018). The SFLA-based GMPPT slows down the speed of both explorative and exploitative search behavior by using the grouping concept. This mechanism increases the global search ability, but requires more particles and long time for the search process.

3.1.3 Artificial bee colony algorithm

Inspired by the natural bee colony work distribution, the bees are divided into employed bees, onlooker bees, and scouts in the ABCA. The feasible solutions are represented by the location of bees (Nakrani and Tovey, 2004). Employed bees take their memories to locate a food supply in the vicinity and convey this information with onlooker bees. Onlooker bees exploitatively search a food source. The employed bee of which the source has been abandoned will turn to a scout bee and starts to search for a new possible origin of food randomly (Karaboga and Akay, 2009).

In the initial stage of the ABCA, the nectar source is randomly generated, and the number is equal to the employed bees. The movement of the employed bees is defined in Eq. 7.

$$v_i^{t+1} = x_i^t + \mathcal{R}_{-1,1} \left(x_i - x_k \right) \quad (7)$$

where x_k is the nearby nectar, x_i is the current nectar. The resulting possible solutions will be compared with the old solutions, and a greedy selection strategy will be used to retain the better solutions. Each onlooker bee selects a nectar source based on probability which is given in Eq. 8.

$$p_i = \frac{\mathcal{F}_i}{\sum_{n=1}^{Np} \mathcal{F}_n} \quad (8)$$

The ABCA integrated perturbation and observation (ABCA-P&O) MPPT algorithm is utilized in (Pilakkat and

Kanthalakshmi, 2020) for GMPPT. It should be noted that increasing the population size to improve performance is not the best option, as this will significantly increase the tracking time. The *Limit* parameter is used to control the transition from employed bees to scout bees. When the *Limit* is small, the GMPPT process has stronger randomness and slower convergence speed. When the *Limit* is large, the movement direction of the colony is mainly dominated by the greedy algorithm, and it is easy to fall into the LMPPs. In Soufyane Benyoucef et al. (2015), an ABCA based GMPPT method was proposed. Compared to the conventional MPPT schemes such as the P&O and InC, it increases the exploitative search ability. In Sundareswaran et al. (2015b), it is shown that the ABCA has a better tracking efficiency than the PSO and enhanced P&O (EPO) methods under the benchmark performance test. The main drawback of the ABCA is the unproductive behavior in exploitation (Jadon et al., 2017). In Fathy (2015), proposed a modified artificial bee colony (MABC) algorithm with an inertia weight formula for the food position to avoid the local sub-optimal solution. Compared with the genetic algorithm (GA), PSO, and ABCA results, the proposed MABC has a higher efficiency. D Pilakkat et al. Pilakkat and Kanthalakshmi (2019) proposed a modified P&O based MPPT scheme by integrating ABCA in the first stage and P&O algorithm in the second stage. As a result, P&O's local search capability and ABC's global search capability are successfully integrated to create the converter's optimum duty cycle in a quick and efficient manner.

3.1.4 Cuckoo search

CS was developed by Yang et al. in 2009 (Yang and Deb, 2009; Mareli and Twala, 2018). In nature, cuckoos lay their eggs in the nests of other birds which can engage in direct conflict with the intruding cuckoos. This is called the holoparasite. Each cuckoo in the CS lays one egg at a time and deposits it in a nest chosen at random. The top-notch egg nests will be passed on to the next generation. The number of available host nests is a fixed value. The host bird discovers the cuckoo's egg with a predetermined probability. The host bird can toss the egg and start again with a fresh nest (Yang and Deb, 2013).

The cuckoo's nesting path and location update formula is given in Eq. 9.

$$x_i^{t+1} = x_i^t + \alpha \times L(\lambda) \tag{9}$$

where α is the step size, and $L(\cdot)$ submitted to Lévy flight function, is given in Eq. 10.

$$L(s) = \frac{u}{|v|^{1/1.5}} \tag{10}$$

Among them, u and v come from the normal distribution as shown in Eq. 11.

$$u \sim N\left(0, \left\{\frac{\Gamma(1+\beta) \times \sin\left(\frac{\pi\beta}{2}\right)}{\Gamma\left[\left(\frac{1+\beta}{2}\right)\right] \times \beta \times 2^{(\beta-1)/2}}\right\}^{2/\beta}\right) \tag{11}$$

$$v \sim N(0, 1)$$

where Γ denotes the gamma function, which is the extension of the factorial function in the real and complex fields (Mosaad et al., 2019). The above-mentioned Lévy flights is the foundation of many other optimization methods. Many insects and animals move over a long distance with various distance steps. The Lévy flight may be used to effectively imitate this feature (Pavlyukevich, 2007).

The CS enjoys several advantages including fast convergence, high efficiency and few tuning parameters. In Ahmed and Salam (2014), a CS-based MPPT scheme with partial shading capability was proposed. In 2019, Mosaad et al. (2019) investigated the GMPPT of PV system based on the CS algorithm. Compared with the neural network and incremental conductance approach, the CS can track the GMPP under various atmospheric conditions with lower power losses. The improvement of CS performance is mainly due to Lévy flights, where the step size is a heavy-tailed distribution. In the Lévy flight, the step sizes comply with the power law. This feature enhances global search performance of the CS-based GMPPT.

3.1.5 Firefly algorithm

Yang et al. proposed the FA (Yang, 2009). The main rule followed by FA is the light intensity emitted by fireflies at a specific distance r that follows the inverse square law. In other words, the light intensity is $I \propto 1/r^2$ at the distance r. The view of a single firefly is limited to several hundred meters at night because the air absorbs light. Inspired by fireflies, the brightness can be correlated with the objective function, and then the firefly groups are sorted according to the brightness of each firefly from smallest to largest. The Euclidean distance between the ith and the jth fireflies is r_{ij}. The attraction of these two individuals is defined as $\beta = \beta_0 \exp(-\gamma r^2)$. The FA compares the brightness of any two fireflies in the population. If $I_i < I_j$, the firefly i will fly towards the firefly j as shown in Eq. 12.

$$x_i^{t+1} = x_i + \beta_0 e^{-\gamma r_{ij}^2}\left(x_j^t - x_i^t\right) + \mathcal{R}_{0,1}\epsilon_i^t \tag{12}$$

where β_0 is the attractiveness at $r = 0$, the randomization $\epsilon_i e^t$ can be easily extended to other distributions such as Lévy flights.

The firefly algorithm has been criticized for differing from the well-established PSO only in a negligible way (Lones, 2014). The standard FA suffers from high computational time complexity and sluggish convergence (Wang and Liu, 2019). The experimental results of FA are not very stable, and the worse values can deprave the performance of the entire tracking

significantly. The main idea of the FA is that each firefly flies towards the firefly brighter than itself, which will inevitably lead to rapid convergence of the group. When the group is all concentrated in one direction, the search ability of the algorithm will decline rapidly and it will not be able to jump out of the local optimum. In Teshome et al. (2016), introduced the average of the brighter flies to replace the brighter individual in any two couple of fireflies. The Teshome's method can decrease the tracking time and increase the tracking accuracy compared with the original FA.

3.1.6 Harris hawk optimization

The HHO simulates the predation of Harris eagle. It was developed by Heidari et al. (2019). It mainly consists of three parts: the exploration, transition, and exploitation phases.

In the exploration phase, a random number q between 0 and 1 is created. Depending on the q, two strategies as shown in **Eq. 13** are possible.

$$X^{t+1} = \begin{cases} X^t_{\text{rand}} - r_1 |X^t_{\text{rand}} - 2r_2 X^t| & q \geq 0.5 \\ \left[X^t_{\text{rabbit}} - X^t_m \right] - r_3 \left[r_4 \times V_{\text{oc, string}} \right] & q < 0.5 \end{cases} \quad (13)$$

where X^t and X^{t+1} are the positions of the hawks in the current and next iteration, X_{rand} is a random hawk, X_{rabbit} is the position of rabbit, r_1, r_2, r_3, r_4 are $\mathcal{R}_{-1,1}$, and X_m is the central position of the current hawks population.

The HHO switches between different behaviors according to the escape-energy of the rabbit. Escape-energy is defined in **Eq. 14**.

$$E = 2E_0 \left(1 - \frac{t}{MaxItr} \right) \quad (14)$$

where E is the escaping energy of the rabbit, and E_0 is the initial state of the energy at the beginning of each iteration, and its value is random generated within [0,1].

In the exploitation phase, there are four behaviors for the generation of the new position of the hawks: soft besiege (SB), hard besiege (HB), soft besiege with progressive rapid dives (SB-PRD), and hard besiege with progressive rapid dives (HB-PRD). The choice of these behaviors relies on the generation of random numbers and E. The SB and HB are the simple updating of the hawks' position according to **Eqs 15**, **16**, respectively.

$$X^{t+1} = X^t_{\text{rabbit}} - X^t - E|JX^t_{\text{rabbit}} - X^t| \quad (15)$$

$$X^{t+1} = X^t_{\text{rabbit}} - X^t - E|\delta X(t)| \quad (16)$$

Lévy flight is introduced to produce the step for the SB-PRD and HB-PRD process as shown in **Eqs 17**, **18**, respectively.

$$X^{t+1} = X^t_{\text{rabbit}} - X^t - E|JX^t_{\text{rabbit}} - X^t| + \mathcal{R}_{0,1} \times L \quad (17)$$

$$X^{t+1} = X^t_{\text{rabbit}} - X^t - E|\delta X(t)| + \mathcal{R}_{0,1} \times L \quad (18)$$

The HHO-based MPPT method for PV systems under PSCs was proposed in Mansoor et al. (2020). Large spikes in the tracking curves occur as a result of the early investigation of the search space for the HHO-based MPPT control. The cause of this phenomena is that the worst solution always exists and has an impact on the tracking process's convergence. Despite this problem, experiments showed that the HHO can obtain better results than P&O and PSO through field atmospheric data and case studies.

3.1.7 Flower pollination optimization

FPO can be concluded into the following two parts: abiotic pollination and biotic pollination (Yang, 2012). In FPO, the biotic is viewed as a global pollination process involving Lévy flights by pollinators. A certain switch probability $p \in [0, 1]$ is used to control the local pollination (explotitative search) and global pollination (explorative search).

At each iteration of FPO, a random number $\mathcal{R}_{0,1}$ is generated. If $\mathcal{R}_{0,1}$ is smaller than the switch probability p, the global pollination described in **Eq. 19** will be carried out.

$$x^{t+1} = x^t + L(g - x^t) \quad (19)$$

where L is a step size drew from the Lévy flight, g is the best individual discovered among all solutions. If $\mathcal{R}_{0,1}$ is larger than the proximity probability p, local pollination described in **Eq. 20** will be carried out.

$$x^{t+1} = x^t + \mathcal{R}_{0,1} \left(x^t_j - x^t_k \right) \quad (20)$$

where x^t_j and x^t_k are pollen from multiple blooms of the same type of plant.

Only two parameters are needed in FPO. In Diab and Rezk (2017) and Samy et al. (2019), the results of a complete evaluation of the FPO-based GMPPT versus DE and PSO with two distinct PV string configurations reveal that the FPO has the highest efficiency. Many researchers tried to improve the tracking speed of the FPO by the introduction of random factors. In Sundararaj et al. (2020), Cauchy preferential crossover is utilized to accelerate the FPO. As a result, the steady-state oscillations are reduced during the MPPT process. Yousri et al. (2019) combine the chaos maps with FPO and improve the dependability and stability of the FPO. When compared to FPO, the chaotic FPO (C-FPO) delivers improved tracking efficiency and a 50% reduction in tracking time.

3.2 Human-based algorithms

3.2.1 Teaching learning based optimization

The TLBO algorithm was created by Rao et al. in 2011 (Rao et al., 2012). No algorithm-specific parameters need to be tuned when using the TLBO. Two basic learning modes, learning through teachers (teacher phase) and learning through

communication with other students (learner stage), are used to describe the TLBO. In TLBO, a population refers to a group of students. The student's score is similar to the fitness value of the optimization problem, and is represented by power value in the GMPPT. The individual who gets the best solution for the whole group is considered to be the teacher. In the teaching phase of TLBO, the update equation for the position of each teacher is expressed by **Eq. 21**.

$$x_i^{t+1} = x_i^t + \mathcal{R}_{0,1} \times \left(x_\text{teacher} - \text{TF} \times \sum_{n=1}^{N_p} x_n \right) \qquad (21)$$

where TF $\in [1, 2]$ is a teacher factor, x_teacher is the individual with the best fitness value.

In the learner phase of TLBO, the update equation for the position of each learner is expressed by **Eq. 22**.

$$x_i^{t+1} = x_i^t + \mathcal{R}_{0,1} \times |x_i - x_j| \qquad (22)$$

where x_j is a randomly selected learner with $i \neq j$. In TLBO, x_i^t will update only if x_i^{t+1} is better than x_i^t for both teacher phase and learner phase.

The algorithm-specific parameters are not required by TLBO. In Rezk and Fathy (2017), the TLBO is used to find the GMPP for a partially shaded PV system. In the PSCs investigated, the average tracking time of GMPP is decreased by more than 23.8% when compared to PSO. However, the TLBO is easy to fall into the LMPPs (Fathy et al., 2018). An improved teaching-learning-based optimization (I-TLBO) is applied to perform GMPPT in (Chao and Wu, 2016). I-TLBO increases the tracking accuracy and improves the tracking response. The proposed I-TLBO uses an adaptive teaching factor TF which is equal to $P(x_{learner})/P(x_{best})$, where $P(x_{learner})$ is the current power value of the learner and $P(x_{best})$ is the current best power value. The TF in I-TLBO decreases as the distance between the learner and the best candidate decreases, which will greatly strengthen the local search capability.

3.2.2 Jaya algorithm

The Jaya algorithm, named after the victory in Sanskrit, is a heuristic optimization method that does not require any algorithm-specific parameters (Rao, 2016). The foundation of Jaya is the belief that the best option for a particular circumstance should be followed, while the worst solution should be avoided (Rao and Saroj, 2017).

In the Jaya based GMPPT algorithm, the initial solutions are randomly generated in $[0, V_{oc, string}]$. Afterwards, each solution is randomly updated using **Eq. 23**.

$$x_i^{t'} = x_i^t + \mathcal{R}_{0,1} \left(x_\text{best}^t - |x_i^t| \right) - \mathcal{R}_{0,1} \left(x_\text{worst}^t - |x_i^t| \right) \qquad (23)$$

where the subscripts i is the index of candidate solution. The first term $\mathcal{R}_{0,1}(x_\text{best}^t - |x_i^t|)$ drives the current candidate solution x_i^t to the positions that are close to the best solution. Vice

versa, the second term $\mathcal{R}_{0,1}(x_\text{worst}^t - |x_i^t|)$ forces the current candidate solution away from the worst solution. x_i^{t+1} is updated to $x_i^{t'}$ only if $x_i^{t'}$ gets a better fitness value than x_i^t, otherwise it will still be x_i^t. This loop will continue until the *MaxItr* is reached.

The Jaya-based MPPT method was developed by Huang et al. for the PV strings working under PSCs in Huang et al. (2017b). The simulation results show that the Jaya-based method takes fewer iterations to converge to the GMPP and has a higher dynamical tracking efficiency than PSO methods. In Huang et al. (2017a), a prediction model-guided Jaya algorithm was proposed. The iterative search procedure incorporates a cubic-spline-based prediction model to guide the updating of candidate solutions. In the Jaya-based MPPT, the particles are far away from the global worst solution and approach to the optimal global solution. This mechanism accelerates the convergence, but it also makes the Jaya algorithm easily fall into a local optimum.

3.3 Physics-based algorithms

3.3.1 Water cycle algorithm

The WCA simulates the water cycle process in nature. It sets three types of individuals in the population: sea, river and streams. The sea is the optimal individual of the current population, the river is a certain number of good individuals, and the remaining poor individuals are streams (Eskandar et al., 2012). For the application of WCA in GMPPT, N_pop of individuals will be generated. Among them, $N_\text{sr} = 1 + N_r$ is the total number of the river and the sea. $N_\text{stream} = N_\text{pop} - N_\text{sr}$ is the number of streams. **Eq. 24** is given to designate raindrops to the river and sea depending on the intensity of the flow.

$$N_\text{sn} = round \left(| \frac{Cost_n}{\sum_{s=1}^{N_\text{sr}} Cost_s} | \times N_{streams} \right), \ n = 1, 2, \ldots, N_\text{sr} \qquad (24)$$

where N_sn is the number of streams that flow to the specific river or sea, and *Cost* denotes the power value.

During the iteration, the new position of streams and rivers are given in **Eqs 25**, **26**.

$$X_\text{stream}^{t+1} = X_\text{stream}^t + \mathcal{R}_{0,1} \times C \times \left(X_\text{river}^t - X_\text{stream}^t \right) \qquad (25)$$

$$X_\text{river}^{t+1} = X_\text{river}^t + \mathcal{R}_{0,1} \times C \times \left(X_\text{sea}^t - X_\text{river}^t \right) \qquad (26)$$

The WCA introduces an evaporation condition to avoid the problem of falling into a local optimum. If $|X_\text{sea}(t) - X_\text{river}^i(t)| < d_\text{max}$ for any river i, the random new river will be generated to replace the old river i. d_max is a small number and decreases with the iteration shown in **Eq. 27**.

FIGURE 4
V_{err} and P_{acc} test results with different algorithms under **(A)** PSC1: 3S-KC175GT; **(B)** PSC2: 5S-KC175GT; **(C)** PSC3: 7S-KC175GT; **(D)** PSC4: 3S-N224A01; **(E)** PSC5: 5S-N224A01; **(F)** PSC6: 7S-N224A01; **(G)** PSC7: 3S-JH10; **(H)** PSC8: 5S-JH10; **(I)** PSC9: 7S-JH10.
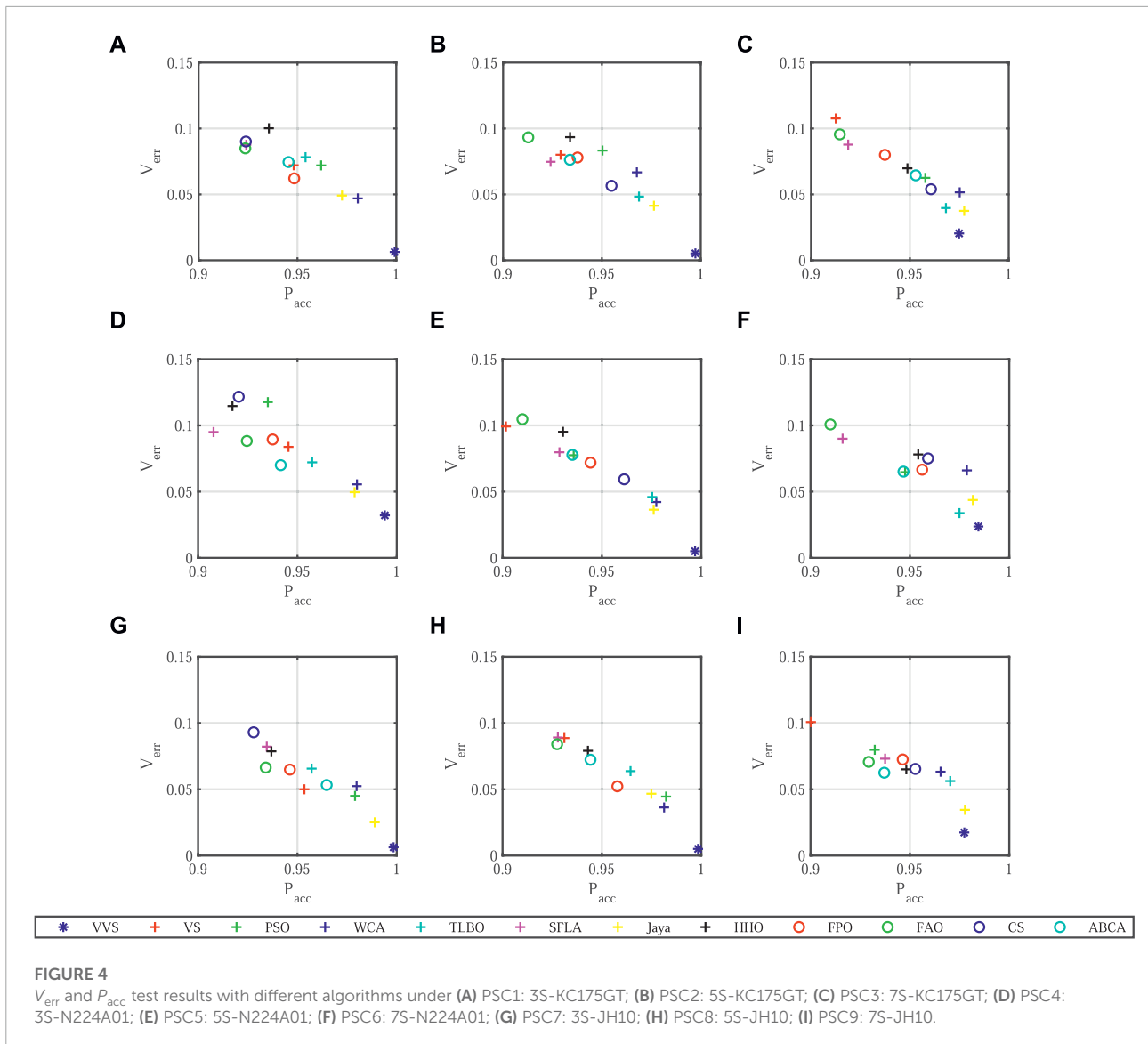
$$d_{max}(t+1) = d_{max}(t) - \frac{d_{max}(t)}{T_{max}} \qquad (27)$$

The WCA-based MPPT is compared with the P&O for PV energy conversion under PSCs in Sarvi et al. (2014). The findings demonstrate that by removing the random number and acceleration coefficients components, the WCA simplifies the MPPT control method. In comparison to P&O, the suggested WCA technique provides exceptional accuracy and speed. However, a large number of individuals are needed to ensure robustness (Heidari et al., 2017).

3.3.2 Vortex search

Vortex search (VS) was proposed by Doğan and Ölmez (2015). The VS is inspired by the vortex pattern created by the flow of the stirred fluid (Ali et al., 2018). In the VS, the

vortex is first centered on the initial center μ_0 as shown in **Eq. 28**.

$$\mu_0 = \frac{V_{oc,string}}{2} \qquad (28)$$

After the generation of the initial solution, the neighbor solutions $C_t(s)$ (initially $t = 0$) are randomly generated around the initial solution μ_0 using a Gaussian distribution as shown in **Eq. 29**.

$$p(x|\mu,\Sigma) = \frac{1}{\sqrt{2\pi|\Sigma|}} exp\left\{ -\frac{1}{2}(x-\mu)^T \Sigma^{-1}(x-\mu) \right\} \qquad (29)$$

where x is the random variable, μ is the sample mean (center of the vortex), and Σ is the con-variance matrix.
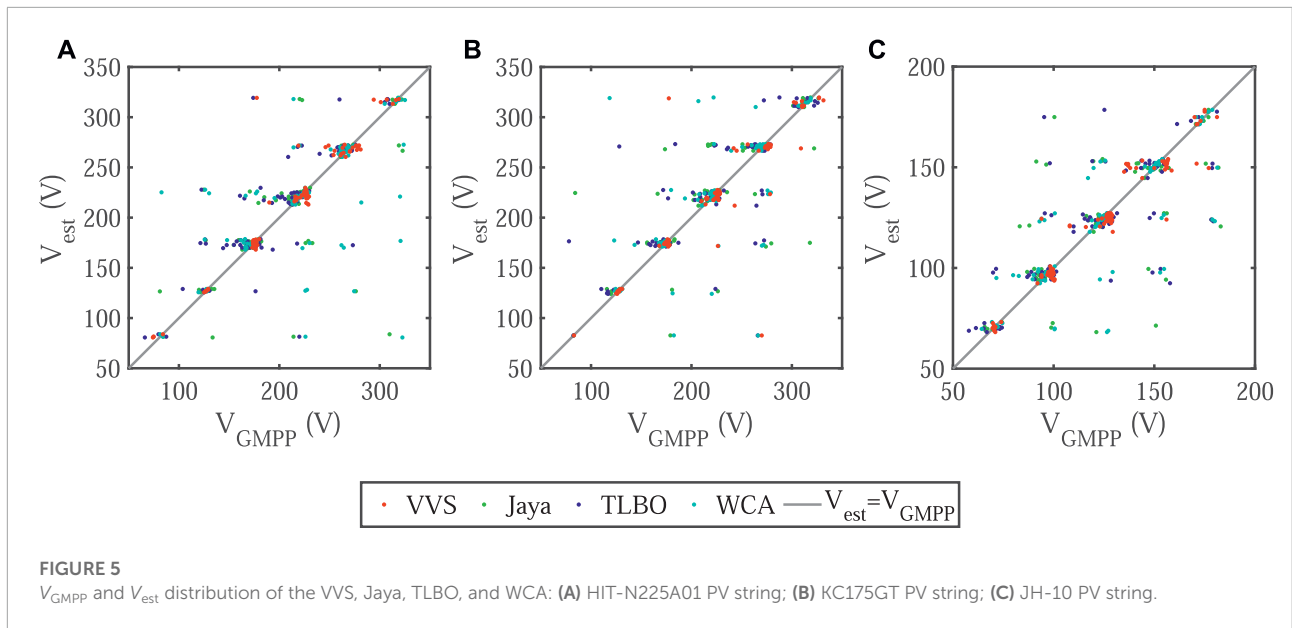
FIGURE 5
V_{GMPP} and V_{est} distribution of the VVS, Jaya, TLBO, and WCA: **(A)** HIT-N225A01 PV string; **(B)** KC175GT PV string; **(C)** JH-10 PV string.

The best solution from $C0(s)$ is chosen in the selection phase to replace the present circle centre $mu0$. The candidate solutions which are outside the search boundaries are shifted inside the boundaries. During each iteration, the inverse incomplete gamma function **Eq. 30** is used to reduce the radius value.

$$\gamma(x, a) = \int_0^x e^{-t} t^{a-1} \, dt \qquad a > 0 \qquad (30)$$

To adjust the resolution, the value of a is equally sampled within [0,1]. For this purpose, the value of a_t is expressed by **Eq. 31** at each iteration.

$$a_t = a_0 - \frac{t}{T_{max}} \qquad (31)$$

where $a_0 = 1$ ensures that the search space is fully covered in the initial iteration.

Algorithm 1 shows the pseudo-code of the VS algorithm. The VS algorithm has some features that are beneficial to the GMPPT process. The VS algorithm ensures convergence by reducing the search radius. Besides, the VS algorithm is simple due to its single-solution-based updating mechanism. However, the integral numerical calculation of incomplete gamma function is a significant challenge for controllers with limited resources. In addition, the VS algorithm does not have the "jump out" mechanism of the current optimal solution. As a result, the selection of initial voltage set-points is important to the VS-based GMPPT algorithm.

Algorithm 1: Description of the VS algorithm Özkış and Babalık (2017).

Input: Initial center μ_0 and initial radius r_0 and their fitness values
Output: Best solution so far s_{best}
1: **for** $i = 1; i < T_{max}; i + +$ **do**
2:   Generate $C_t(s)$
3:   S'=Select($C_t(s)$)
4:   **if** $f(s') > f(s_{best})$ **then**
5:     $s_{best} = s'$
6:     $f(s_{best}) = f(s')$
7:   **end if**
8:   $\mu_{t+1} = s_{best}$
9:   $r_{t+1} = $ Change(r_t)
10:   $t = t + 1$
11: **end for**

3.3.3 Variable vortex search

This paper proposes a variable vortex search (VVS), which balances the exploration and exploitation behaviors by using deterministic initial points and the variable search steps. Its search process can be divided into two steps: pre-search and optimization. The former provide a good estimation of GMPP locus based on the electrical characteristics of a PV string under PSCs, while the latter applies a variable step size strategy to adjust the search radius in exploitative and explorative search.

The pre-search strategy is developed based on the observations of $V_m - V_s$ characteristics. **Figure 3A** indicates the $V_m - V_s$ characteristics of a PV string comprising four modules. The voltage of a working module is non-negative, while a shaded modules obtains a negative voltage. The number of working modules $N_{p,1}$ is equal to 1 at the 1st sampling point. Two additional modules start to work at the 2nd sampling point and the $N_{p,2}$ is increased to 3. The number of newly added working modules at the ith sampling point is denoted by $D_{p,i}$. We can get $N_{p,3} = 4$ and $D_{p,3} = 1$ for the 3rd sampling point.

FIGURE 6
P_{acc} distribution of the algorithms in the test of three JH-10 modules in series connection with random PSCs: **(A)** VVS; **(B)** VS; **(C)** ABCA; **(D)** CS;
(E) FAO; **(F)** FPO; **(G)** HHO; **(H)** Jaya; **(I)** PSO; **(J)** SFLA; **(K)** TLBO; **(L)** WCA.
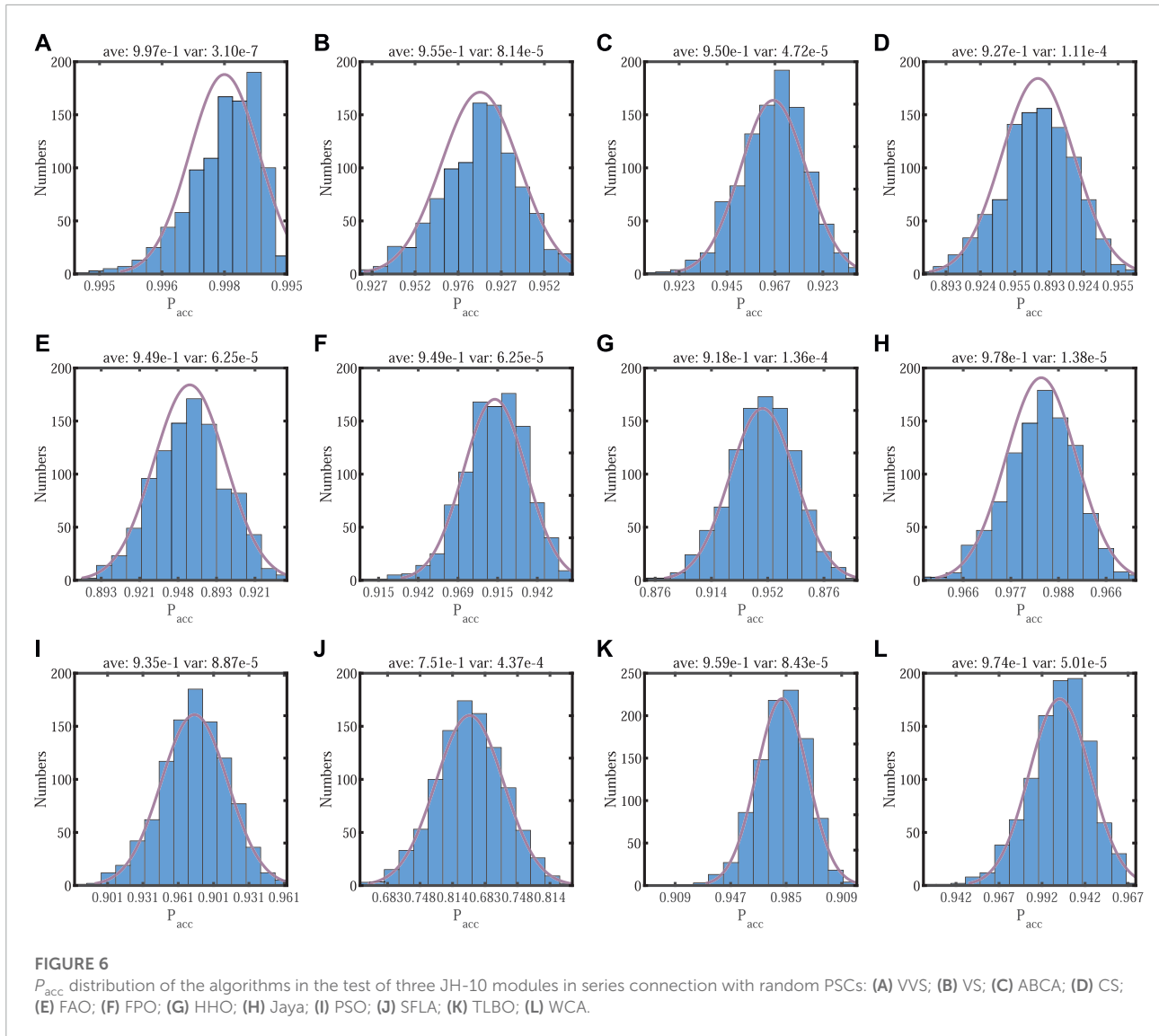
Algorithm 2 pesents the pseudo-code of the pre-search strategy. The pre-search strategy starts from the 1st sampling point, whose voltage is equal to $0.5 \times V_{oc,m}$. The $(i + 1)$th sampling voltage is $(N_{p,i} + 0.5) \times V_{oc,m}$ and this will continue until the $N_{p,i}$ is equal to the number of series-connected PV modules N_m. The pre-search strategy provides a good initial search region for the optimization process. Previous studies show that the MPP voltage is about $0.8 \times V_{oc}$ on a PV module (Xiao et al., 2007; Patel and Agarwal, 2008; Tey and Mekhilef, 2014; Başoğlu, 2018). Therefore, the initial points can be calculated by $(N_{p,i} - D_{p,i} + 0.8 \times D_{p,i}) \times V_{oc,m} = (N_{p,i} - 0.2 \times D_{p,i}) \times V_{oc,m}$. **Figure 3B** shows the locations of sampling points and initial points on the P-V curve. It is observed that these initial points are close to the GMPP and the LMPPs, but the errors can be further reduced by the proposed VVS algorithm.

The pseudo-code of the tracking is shown in Algorithm 3. The best solution from the pre-search results is selected as the current circle center $C_0(s)$ at the first round of selection. Then, a number of solutions $C_{t+1}(s)$ are randomly generated around $C_t(s)$ (t represents the iteration index) by using a Gaussian distribution in the search regions. For the ith vortex, its center will be updated if the new solution gets a larger power value. The radius of the search region for the ith vortex is generated according to **Eq. 32**.

$$r = f \times \mathcal{R}_{-0.5,\,0.5} \times n \times D_{p,i} \times V_{oc,m} \tag{32}$$

where $f = k \times \frac{\sqrt{x^2+x}}{exp(x)}$, $x = \frac{t}{T_{max}}$, $k = \frac{\sqrt{1/2+1/\sqrt{2}}}{exp(1/\sqrt{2})}$. k is approximately equal to 1.85 so that the function f has a maximum value of 1. n is a constant number within [0, 0.5] according to the electrical characteristics of PV modules. $n \times D_{p,i} \times V_{oc,m}$ is the initial radius of the ith vortex. **Figure 3C** illustratives the proces. The function
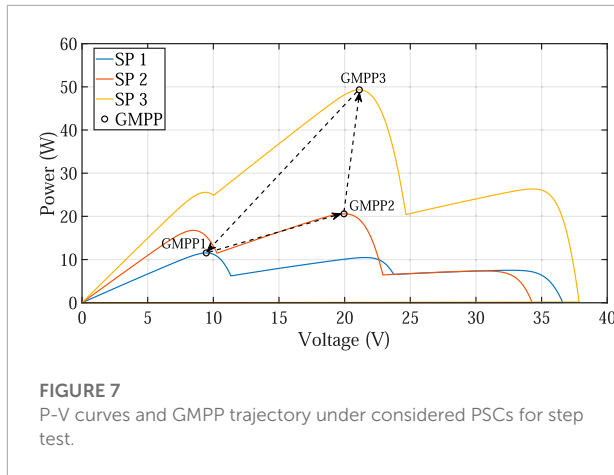
FIGURE 7
P-V curves and GMPP trajectory under considered PSCs for step test.

f is a mountain-like curve and determine the effective radii of the search regions.

The proposed VVS algorithm uses prior knowledge to equilibrate the exploration and exploitation efficiently. At the first step of the search, the initial points of the system are determined according to the PSCs. In the second step, the radii of the search regions are varying over iterations. The VVS uses small search radii to conduct exploitation and followed by large radii to conduct exploration. After such a search process with a variable radius, the approximate location of the GMPP will be determined. Then the radii of the VVS shrink to a small value again to locate the GMPP precisely.

Algorithm 2: Determination of initial points.

Input: Voltage, current information, N_m, and $V_{oc,s}$
Output: Initial points list V_{Init}
1: $V_{oc,m} = V_{oc,s}/N_m$
2: $i = 1$
3: **while** $N_p \leq N_m$ **do**
4:      Calculate $N_{p,i}$ and $D_{p,i}$
5:      Increase the sampling voltage to $(N_{p,i} + 0.5) \times V_{oc,m}$
6:      $i = i + 1$
7: **end while**
8: **for** $j = 1; j \leq i; j + +$ **do**
9:      **if** $D_{p,j} > 1$ **then**
10:         $V_{Init,j} = (N_{p,j} - 0.2 \times D_{p,j}) \times V_{oc,m}$
11:     **else**
12:         $V_{Init,j} = (N_{p,j} + 0.5) \times V_{oc,m}$
13:     **end if**
14: **end for**
15: **return**

Algorithm 3: Description of the VVS-based GMPPT algorithm.

Input: Initial points $C_0(s)$, initial radius R_{Init}, and the best power value found so far s_{best}
Input: Number of initial points IndNum and maximum iteration number T_{max}
Output: Maximum power value so far s_{best}
1: **for** $t = 1; t < T_{max}; t + +$ **do**
2:      $x = t/\text{MaxItr}$
3:      $f = k \times \sqrt{x^2 + x}/exp(x)$
4:      **for** $i = 1; i < \text{IndNum}; i + +$ **do**
5:          $s' = s_i + f \times rand \times n \times D_{p,i} \times V_{oc,m}$
6:          **if** $P(s_i) > P(s_{best}) - PowTolerance$ and $t > 0.5 \times T_{max}$ **then**
7:              Discard vortex s_i
8:              IndNum=IndNum-1
9:          **else if** $P(s_i) < P(s_{best})$ **then**
10:             $s_{best} = s_i$
11:             $s_i = s'$
12:         **end if**
13:     **end for**
14: **end for**

4 Simulation and experimental analysis

4.1 Metrics of tracking performance

Six performance metrics, namely, tracking accuracy of power P_{acc}, tracking efficiency of power P_{eff}, minimum tracking time T_{min}, mean squared error of voltage V_{MAE}, root mean square error of voltage V_{RMSE}, and normalized tracking error of the voltage V_{err} were used in the tracking performance evaluation. $P_{acc}, P_{eff}, T_{min}, V_{MAE}, V_{RMSE}$ and V_{err} are expressed by **Eqs 33–38**.

$$P_{acc} = \frac{P_{est}}{P_{GMPP}} \tag{33}$$

$$P_{eff} = \sum_{i=1}^{N_{step}} \frac{P_i}{P_{GMPP}} \tag{34}$$

$$T_{min} = \frac{N_{best}}{N_{step}} \tag{35}$$

$$V_{MAE} = \frac{1}{m} \sum_{i=1}^{m} |V_{GMPP,m} - V_{est,m}| \tag{36}$$

$$V_{RMSE} = \sqrt{\frac{\sum_{i=1}^{m}(V_{GMPP,m} - V_{est,m})^2}{m}} \tag{37}$$

$$V_{err} = \frac{\sum_{i=1}^{m} |V_{GMPP,m} - V_{est,m}|/V_{oc,string,m}}{m} \tag{38}$$

where P_{est} is the estimated power value, P_{GMPP} is the global maximum power value, P_i is the output power of PV string in step i, N_{best} is the iteration index when the output power reaches 95% of P_{est}, m is the number of test sets, $V_{GMPP,m}$ is the real GMPP voltage in the mth scene, $V_{oc,string,m}$ is the open-circuit voltage of the PV string in the mth scene, and $V_{est,m}$ is the estimated MPP voltage in the mth scene. In Mamarelis et al. (2014), the accuracy of GMPPT P_{acc} is also called steady-state MPPT efficiency. P_{eff} is used in Chaieb and Sakly (2018) to represent the efficiency of the tracking process. In da Rocha et al. (2020), the P_{eff} is also called the tracking factor (TF). T_{min} is proposed in this paper to evaluate the prematurity. If P_{acc} and T_{min} are small at the same time, it indicates that the GMPPT algorithm has fallen into the local optimum.

4.2 Software simulation

Simulation studies were conducted in Matlab/Simulink to perform a comprehensive evaluation. The PV string's load is
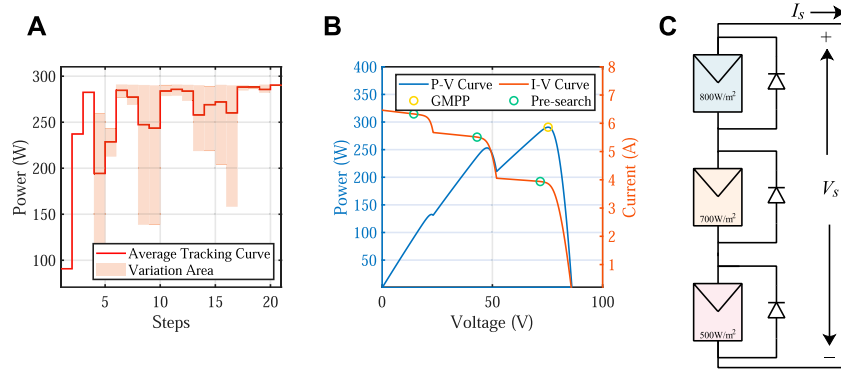
FIGURE 8
Average and best power curves under considered PSC test of a PV string with 3 PV modules: **(A)** Average tracking power curve and variation area; **(B)** P-V and I-V curve of the tested PSC; **(C)** The PV string topology.
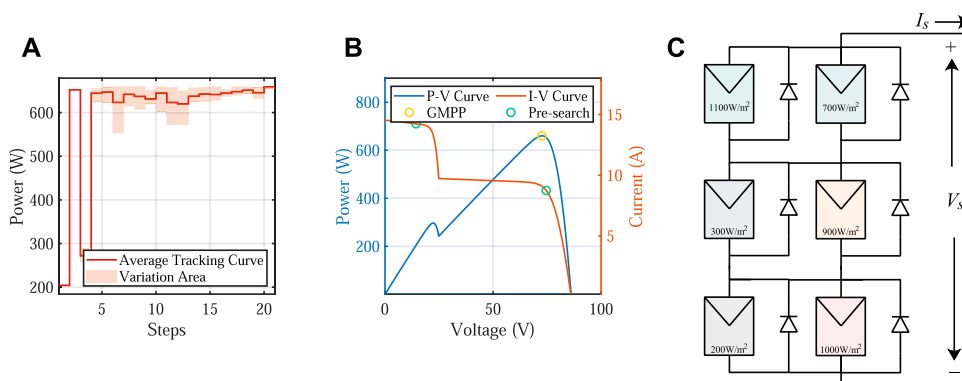
FIGURE 9
Average and best power curves under considered PSC test of a PV array with 3*2 PV modules connected in TCT topology: **(A)** Average tracking power curve and variation area; **(B)** P-V and I-V curve of the tested PSC; **(C)** The PV array topology.

considered as a controllable voltage source. Different PV strings (monocrystalline, polycrystalline, and thin-film) with 3, 5, 7 series-connected modules are used in the simulation. **Table 1 Table 2** shows the specifications of the PV modules. Each data-set contains 100 random PSCs (G = [100, 1100]W/m², T = 25°C).

To make a fair comparison, the maximum sampling number for all the GMPPT algorithms is set to 20. The average test results of each data-set are shown in **Table 3**. Each experiment was conducted 100 times, and then the average value was taken as the final result. The proposed VVS-based GMPPT method obtains the highest accuracy according to the V_{MAE} and V_{RMSE}. Although VS, PSO and WCA show a competitive P_{eff} with the VVS-based GMPPT methods, they fall into the LMPPs because their tracking accuracy is relatively low. In addition, the V_{err} and P_{acc} test results of each data-set are shown in **Figure 4** where the vertical axis represents P_{eff} and the horizontal axis represents P_{acc}. The superiority of the proposed algorithm can be seen intuitively. The

VVS owns the smallest V_{err} in all cases among all algorithms. In the PSC3, PSC6, and PSC9, the Jaya, TLBO, and WCA show a competitive P_{acc} with the VVS-based GMPPT methods. The Jaya, TLBO, and WCA fell into the LMPPs due to the lack of exploration. To further illustrate the prematurity phenomenon, the V_{GMPP} and V_{est} distributions of the VVS, Jaya, TLBO, and WCA in the test of seven HIT-N225A01, KC175GT, and JH-10 modules in series connection with random PSCs are shown in **Figure 5**. The distribution of the V_{est} from the VVS test results is more concentrated around the grey line ($V_{est} = V_{GMPP}$) than that of the other algorithms. It indicates that the VVS made a good balance between the explorative and exploitative searching behavior.

The probability distributions were collected in order to describe the impact of random factors. Each algorithm was tested 1000 times with the data-set created from a 3-series-connected JH-10 PV string under 100 randomly generated PSCs. The P_{acc} distributions of each algorithm are shown in **Figure 6**.

FIGURE 10
The power and voltage tracking trajectories of the 12 different algorithms in the step test: **(A)** VVS; **(B)** VS; **(C)** ABCA; **(D)** CS; **(E)** FAO; **(F)** FPO; **(G)** HHO; **(H)** Jaya; **(I)** PSO; **(J)** SFLA; **(K)** TLBO; **(L)** WCA.
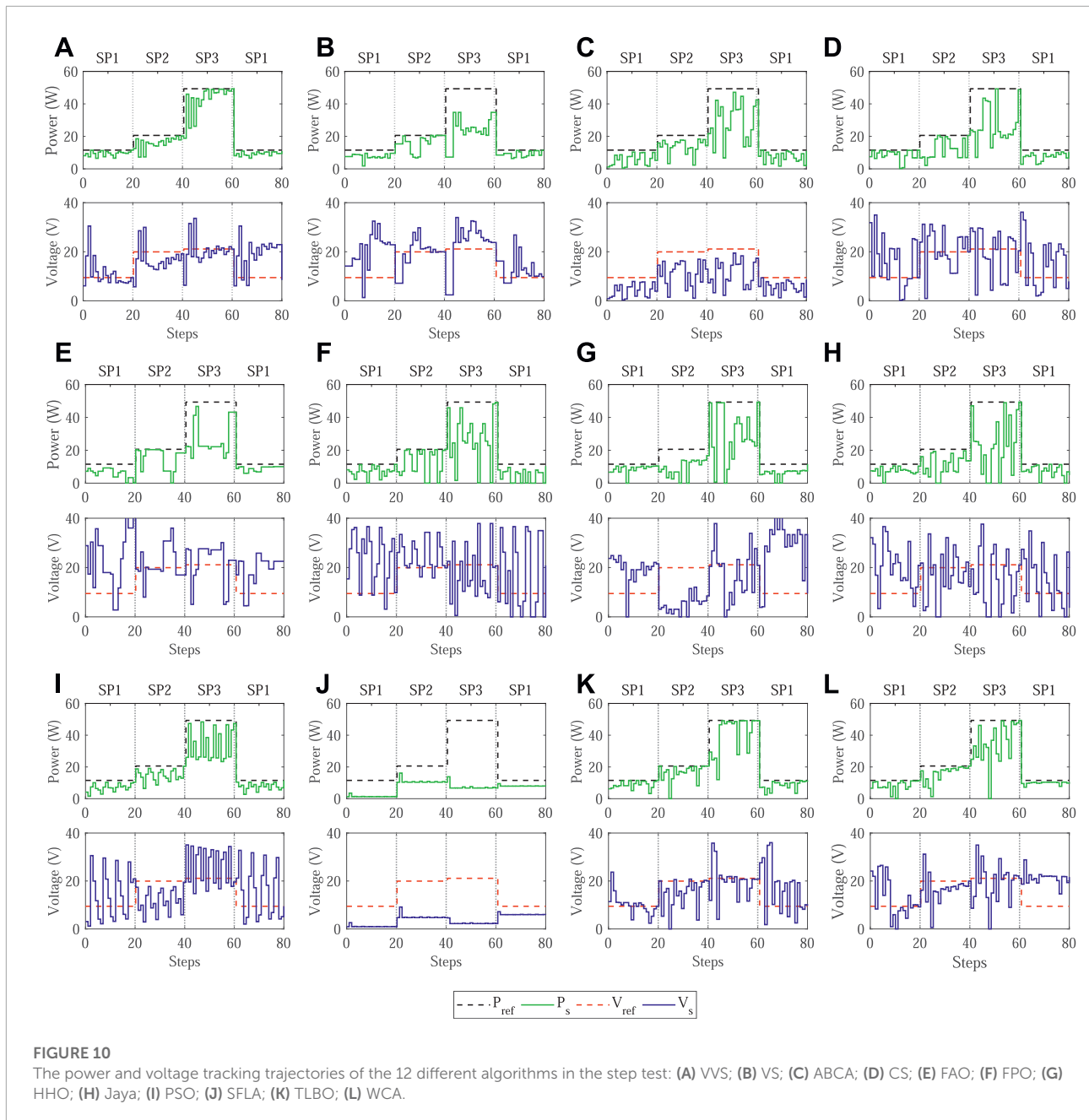
Among all the algorithms, the VVS-based GMPPT method produced the P_{acc} results with the highest average of 0.997 and the smallest variance of 3.10e-7. Compared to the VS algorithm, the proposed VVS improved the P_{acc} by nearly 4% according to **Figures 6A,B**.

All methods were tested under highly fluctuating atmospheric conditions for their dynamic performance test. The shading patterns (SPs) and the corresponding P-V curves are listed in and **Figure 7**, respectively. The location of the GMPP varies from GMPP1 to GMPP3, then ends in GMPP1.

A PV string with 3 modules, and a PV array with 3*2 total cross tied configuration (TCT) modules are used to test the static performance of the proposed algorithm. The test results are shown in **Figures 8**, **9**, separately. The proposed algorithm was run 10 times and the test results were averaged to eliminate the influence of random factors on system performance. The red area presented in **Figures 8A**, **9A** denotes the variation area of power during the tracking process. From this, we can see that with the increase in the number of iterations, the VVS algorithm proposed in this paper gradually converges the search radius until the GMPP is determined.

FIGURE 11
Distribution of the voltage sampling points for the algorithms in the test of three JH-10 modules in series connection with random PSCs: **(A)** VVS; **(B)** VS; **(C)** ABCA; **(D)** CS; **(E)** FAO; **(F)** FPO; **(G)** HHO; **(H)** Jaya; **(I)** PSO; **(J)** SFLA; **(K)** TLBO; **(L)** WCA.
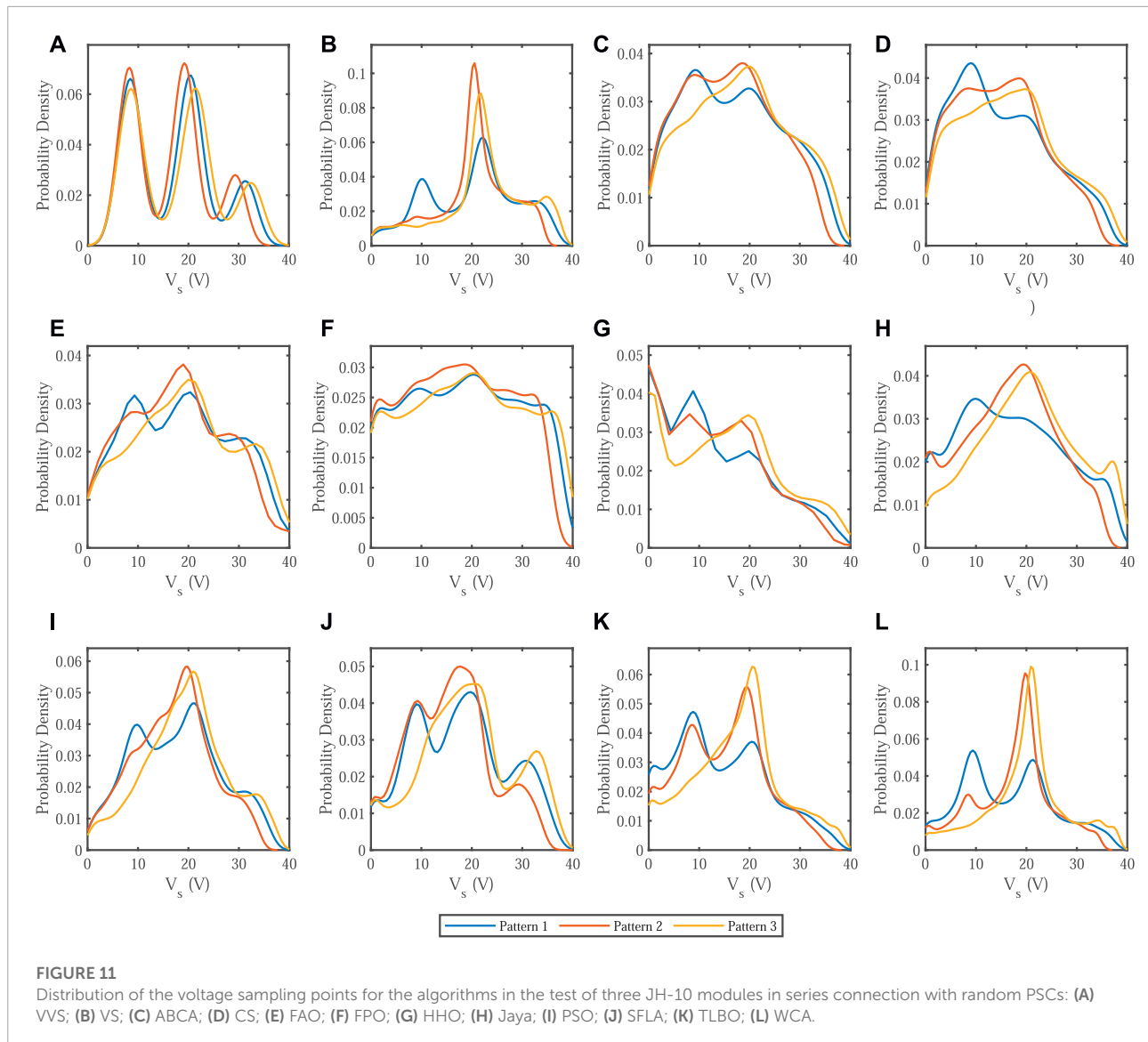
The simulation results from the VVS-based GMPPT is depicted in **Figure 10A** and it shows that the VVS has tracked the GMPP on every pattern. **Figure 10B** reveals that the VS algorithm was tracked in a LMPP in the first SP1. The performance evaluation results of the other methods are shown in **Figure 10**. It can be seen that the priority of exploration is higher than exploitation in the ABCA and CS-based GMPPT. The HHO, Jaya, WCA, and SFLA cannot track the real GMPP under the SP1, where two different LMPPs with similar power values appeared. Based on the aforementioned P_{acc} distribution analysis, it can be concluded that the key to improve GMPPT performance lies in the balance of exploitative and explorative search capabilities.

Figure 11 shows the probability density estimation of the voltage sampling points during the MPPT process. For each algorithm under the PSC1-3 shown in **Table 1**, the data contains 1000 (runs) × 20 (steps) voltage sampling points. It can be observed that the distributions of the voltage sampling points from proposed VVS-based methods agree with the distribution of LMPPs. Besides, the VVS-based GMPPT method obtains a relatively narrow distribution compared with the VS-based GMPPT method. The test results show that the variable step size and the deterministic starting points can result in a multi-modal distribution that is the same as the LMPPs distribution when the PV modules receive different levels of solar irradiance.

FIGURE 12
Test results with different algorithms under PSC: **(A)** Best fitness value during the tracking process; **(B)** Polynomial curve fitted best fitness value (solid line) and average fitness value (dash line) during the tracking process; **(C)** I-V and P-V characteristics.

FIGURE 13
Overview of experimental setup.
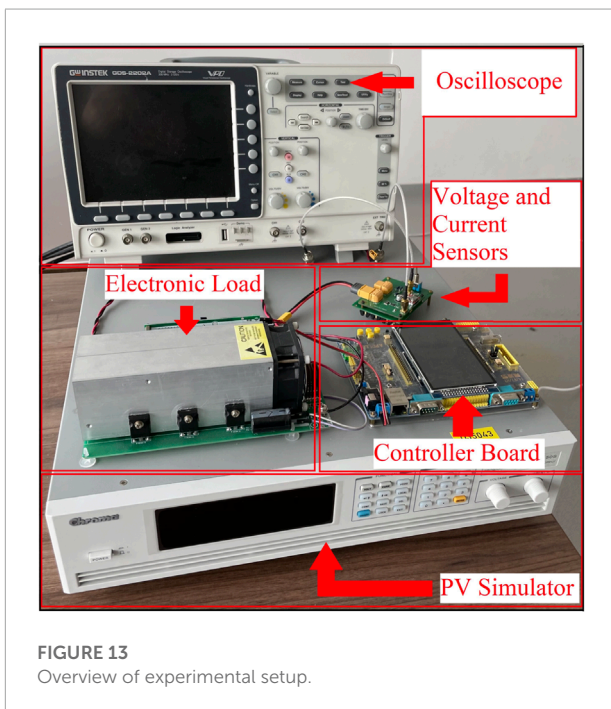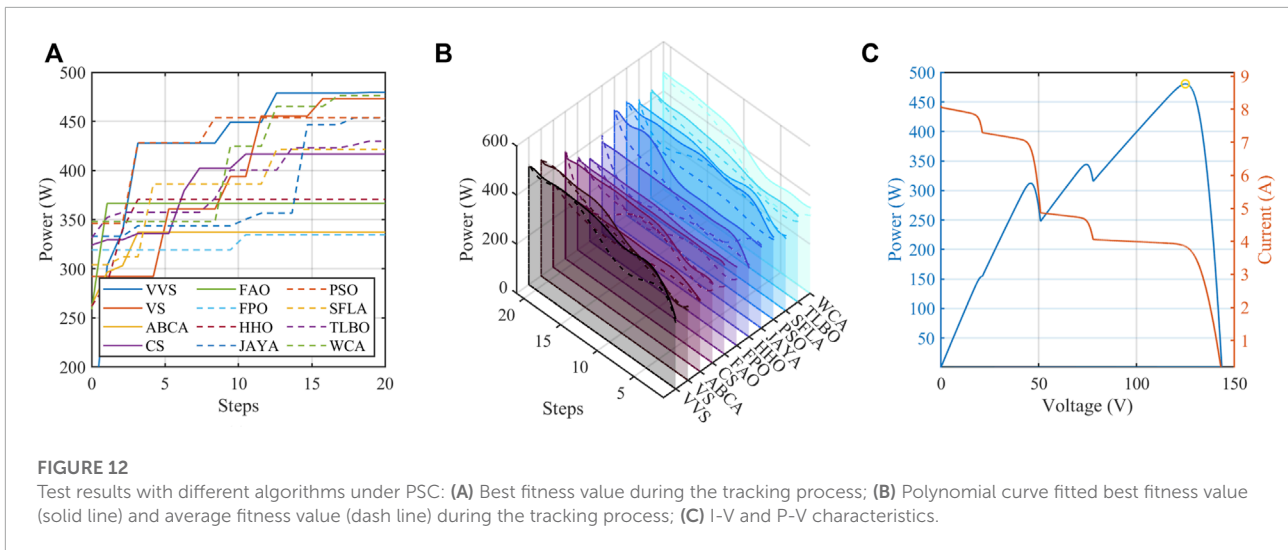
Figure 12 shows the test results obtained from different algorithms under the specified PSC. **Figure 12A** shows the average best fitness value (maximum power) of different algorithms during the tracking process of 20 steps. The proposed VVS-based algorithm successfully tracked the GMPP. The SFLA and WCA based algorithms trapped in the LMPP with 320W. The CS and FAO based algorithms trapped in the LMPP with 340W. **Figure 12B** shows the polynomial curve fitted best fitness

value (solid line) and average fitness value (dash line) during the tracking process. There is almost same continuous growth trend for the proposed VVS-based algorithm, which explains the robustness and stability of the algorithm. **Figure 12C** shows the I-V and P-V characteristics of this PSC.

4.3 Hardware evaluation and implementation

The experimental hardware system is shown in **Figure 13**. A solar PV string emulator (Chroma 62020H) was used to generate the required P-V and I-V characteristics. A micro-controller unit (STM32F103), was opted for the processor of the system. The oscilloscope (GW Instek GDS-2202A) was used to collect signals (P_{pv}, I_{pv}, V_{pv}) from the sensor board. The programmable load (SOUSIM 300W) adjusted the operating voltage of the PV emulator in constant voltage mode.

The tracking waveform of the VVS-based GMPPT is shown in **Figure 14A**. The proposed VVS algorithm has a faster convergence speed than other algorithms. It is worthy pointing out that the 100 sampling points is enough for almost all the tested algorithms. The VVS-based GMPPT methods takes 1.3s, achieved the best result in the test bench.

Experiments were carried out in a rooftop PV system as shown in **Figure 15** to further confirm the validation of the proposed technique. The PV string was connected to a DC electronic load (in constant voltage mode). A host PC was used to control the electronic load. An oscilloscope was used to collect the I_{pv} and V_{pv} signal from the current probe and the voltage probe. **Figure 16** shows the typical tracking waveforms.

FIGURE 14
Voltage, current, and power tracking trajectories of the methods under PSC: **(A)** VVS; **(B)** VS; **(C)** ABCA; **(D)** CS.

FIGURE 15
Hardware evaluation platform.

FIGURE 16
Tracking waveforms.
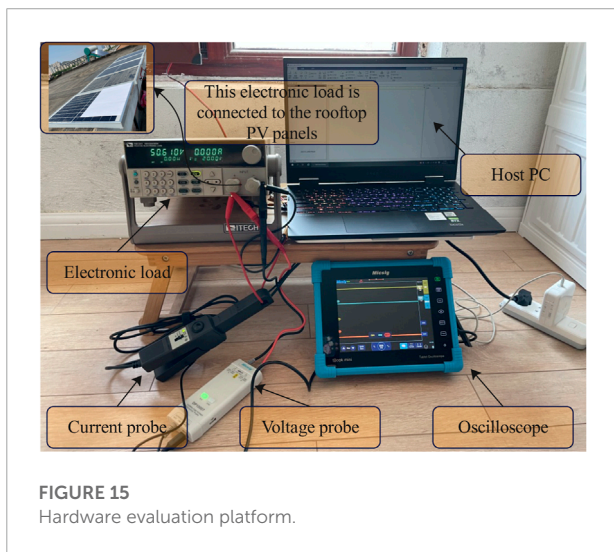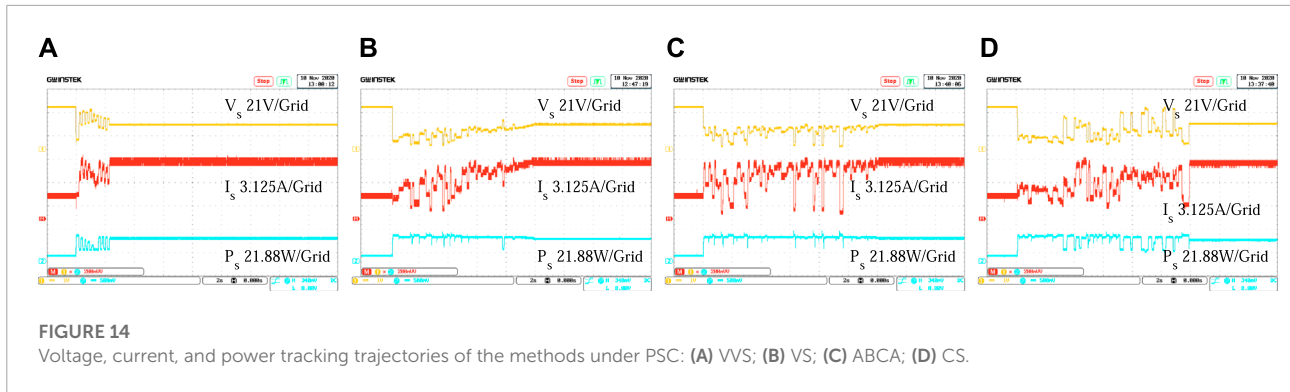
It shows the proposed algorithm consisting of three particles. The decrease in the search radius makes the tracking algorithm converge to the GMPP point with $V_{pv} = 42.821V$, $I_{pv} = 0.387A$ and $P_{pv} = 16.575W$.

Random number generation is an important part of the heuristic algorithms (Darwish, 2018). In the hardware test, the micro-controller uses an analog-to-digital (AD) pin to collect the last 4 bits of power supply noise as the seed to generate the random numbers. The uniformly distributed numbers within the range of $[0, 1]$ or $[−1, 1]$ are needed for the PSO, SFLA, ABCA, WCA, Jaya, HHO, and TLBO. This can be achieved by *rand* function in C code. In the VS and VVS, the normal distribution is needed. The CS, FAO and FPO apply Lévy flight, which requires two random number within the normal distribution. Each random method was conducted 1000 times in the STM32F103RCT6 micro-controller at 72 Mhz core clock frequency to evaluate the computational cost of the uniform distribution, normal distribution, and Lévy flight. The time cost for a 100 uniformly distributed number was 0.166 ms. As for the normal distribution, Box–Muller method takes 23.04 ms. 12.20, 18.68 and 31.64 ms were needed for 25, 50 and 100 sampling numbers when the micro-controller used the law of large numbers (Yao and Gao, 2015) to generate normal distribution. The Marsaglia method was used for normally-distributed numbers, and it costs 17.24 ms. Due to the complexity of floating-point arithmetic, the Lévy flight takes 94.08 ms, which was a longer time than the generation of same quantities of random numbers in uniform or normal distribution.
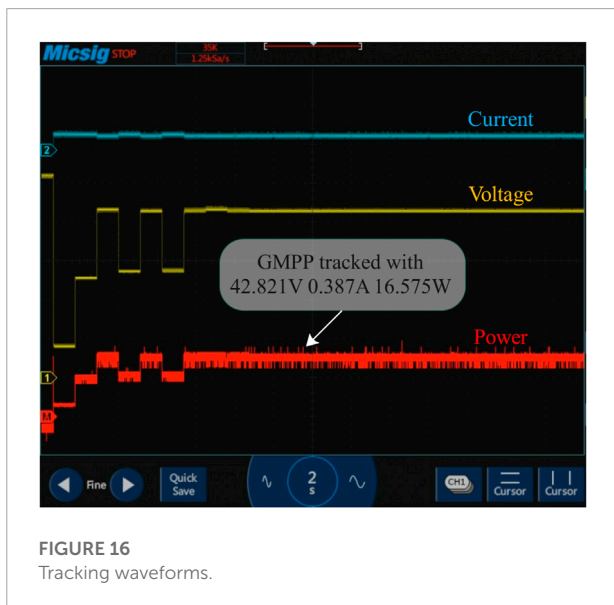
5 Conclusion

In this paper, the challenges in twelve heuristic-optimization-based GMPPT techniques, especially the exploitative and explorative search capabilities, have been analyzed by a comprehensive study. A novel VVS-based GMPPT method, which is capable of improving the performance of GMPPT

by using variable step size and deterministic starting points, is proposed in this paper. In the simulation and hardware tests, the tracking accuracy of the proposed VVS-based GMPPT is more than 99% and its tracking efficiency is the best among all tested methods. Moreover, it reduces the computational burden and is easy to implement. The discussion and analysis of the most important and current heuristic optimization methods developed in the literature, as well as the newly suggested VVS-based GMPPT approach, will allow researchers to choose the best method for their preferences and priorities.

Data availability statement

The datasets presented in this study can be found in online repositories. The names of the repository/repositories and accession number(s) can be found below: https://github.com/KangshiWang/PV_Comparative_Study.

Author contributions

KW: methodology, investigation, and writing-original draft preparation. JM: supervision and writing- original draft preparation. KM: supervision and project administration. KH and XH: review editing.

Conflict of interest

The authors declare that the research was conducted in the absence of any commercial or financial relationships that could be construed as a potential conflict of interest.

Publisher's note

All claims expressed in this article are solely those of the authors and do not necessarily represent those of their affiliated organizations, or those of the publisher, the editors, and the reviewers. Any product that may be evaluated in this article, or claim that may be made by its manufacturer, is not guaranteed or endorsed by the publisher.

References

Ahmad, R., Murtaza, A. F., and Sher, H. A. (2019). Power tracking techniques for efficient operation of photovoltaic array in solar applications–a review. *Renew. Sustain. Energy Rev.* 101, 82–102. doi:10.1016/j.rser.2018.10.015

Ahmed, J., and Salam, Z. (2014). A maximum power point tracking (mppt) for pv system using cuckoo search with partial shading capability. *Appl. Energy* 119, 118–130. doi:10.1016/j.apenergy.2013.12.062

Ahmed, N. A., Abdul Rahman, S., and Alajmi, B. N. (2021). Optimal controller tuning for p&o maximum power point tracking of pv systems using genetic and cuckoo search algorithms. *Int. Trans. Electr. Energy Syst.* 31, e12624. doi:10.1002/2050-7038.12624

Ali, W., Qyyum, M. A., Qadeer, K., and Lee, M. (2018). Energy optimization for single mixed refrigerant natural gas liquefaction process using the metaheuristic vortex search algorithm. *Appl. Therm. Eng.* 129, 782–791. doi:10.1016/j.applthermaleng.2017.10.078

Atems, B., and Hotaling, C. (2018). The effect of renewable and nonrenewable electricity generation on economic growth. *Energy Policy* 112, 111–118. doi:10.1016/j.enpol.2017.10.015

Bana, S., and Saini, R. (2017). Experimental investigation on power output of different photovoltaic array configurations under uniform and partial shading scenarios. *Energy* 127, 438–453. doi:10.1016/j.energy.2017.03.139

Başoğlu, M. E. (2018). An improved 0.8 v oc model based gmppt technique for module level photovoltaic power optimizers. *IEEE Trans. Ind. Appl.* 55, 1913–1921. doi:10.1109/tia.2018.2885216

Bouraiou, A., Hamouda, M., Chaker, A., Sadok, M., Mostefaoui, M., Lachtar, S., et al. (2015). Modeling and simulation of photovoltaic module and array based on one and two diode model using matlab/simulink. *Energy Procedia* 74, 864–877. doi:10.1016/j.egypro.2015.07.822

Chaieb, H., and Sakly, A. (2018). A novel mppt method for photovoltaic application under partial shaded conditions. *Sol. Energy* 159, 291–299. doi:10.1016/j.solener.2017.11.001

Chao, K.-H., and Wu, M.-C. (2016). Global maximum power point tracking (mppt) of a photovoltaic module array constructed through improved teaching-learning-based optimization. *Energies* 9, 986. doi:10.3390/en9120986

da Rocha, M. V., Sampaio, L. P., and da Silva, S. A. O. (2020). Comparative analysis of mppt algorithms based on bat algorithm for pv systems under partial shading condition. *Sustain. Energy Technol. Assessments* 40, 100761. doi:10.1016/j.seta.2020.100761

Danandeh, M., and Mousavi G., S. (2018). Comparative and comprehensive review of maximum power point tracking methods for pv cells. *Renew. Sustain. Energy Rev.* 82, 2743–2767. doi:10.1016/j.rser.2017.10.009

Darwish, A. (2018). Bio-inspired computing: algorithms review, deep analysis, and the scope of applications. *Future Comput. Inf. J.* 3, 231–246. doi:10.1016/j.fcij.2018.06.001

Deboucha, H., Kermadi, M., Mekhilef, S., and Belaid, S. L. (2021). Voltage track optimizer based maximum power point tracker under challenging partially shaded photovoltaic systems. *IEEE Trans. Power Electron.* 36, 13817–13825. doi:10.1109/tpel.2021.3089658

Diab, A. A. Z., and Rezk, H. (2017). Global mppt based on flower pollination and differential evolution algorithms to mitigate partial shading in building integrated pv system. *Sol. Energy* 157, 171–186. doi:10.1016/j.solener.2017.08.024

Díaz Martínez, D., Trujillo Codorniu, R., Giral, R., and Vázquez Seisdedos, L. (2021). Evaluation of particle swarm optimization techniques applied to maximum power point tracking in photovoltaic systems. *Int. J. Circ. Theor. Appl.* 49, 1849–1867. doi:10.1002/cta.2978

Doğan, B., and Ölmez, T. (2015). A new metaheuristic for numerical function optimization: vortex search algorithm. *Inf. Sci.* 293, 125–145. doi:10.1016/j.ins.2014.08.053

Eberhart, R., and Kennedy, J. (1995). Particle swarm optimization. *Proc. IEEE Int. Conf. neural Netw. (Citeseer)* 4, 1942–1948.

Eltamaly, A. M., Al-Saud, M., Abokhalil, A. G., and Farh, H. M. (2020). Simulation and experimental validation of fast adaptive particle swarm optimization strategy for photovoltaic global peak tracker under dynamic partial shading. *Renew. Sustain. Energy Rev.* 124, 109719. doi:10.1016/j.rser.2020.109719

Eltamaly, A. M. (2021). An improved cuckoo search algorithm for maximum power point tracking of photovoltaic systems under partial shading conditions. *Energies* 14, 953. doi:10.3390/en14040953

Eltamaly, A. M., Farh, H. M., and Othman, M. F. (2018). A novel evaluation index for the photovoltaic maximum power point tracker techniques. *Sol. Energy* 174, 940–956. doi:10.1016/j.solener.2018.09.060

Eskandar, H., Sadollah, A., Bahreininejad, A., and Hamdi, M. (2012). Water cycle algorithm–a novel metaheuristic optimization method for solving constrained engineering optimization problems. *Comput. Struct.* 110, 151–166. doi:10.1016/j.compstruc.2012.07.010

Eusuff, M., Lansey, K., and Pasha, F. (2006). Shuffled frog-leaping algorithm: a memetic meta-heuristic for discrete optimization. *Eng. Optim.* 38, 129–154. doi:10.1080/03052150500384759

Fathy, A. (2015). Reliable and efficient approach for mitigating the shading effect on photovoltaic module based on modified artificial bee colony algorithm. *Renew. Energy* 81, 78–88. doi:10.1016/j.renene.2015.03.017

Fathy, A., Ziedan, I., and Amer, D. (2018). Improved teaching–learning-based optimization algorithm-based maximum power point trackers for photovoltaic system. *Electr. Eng.* 100, 1773–1784. doi:10.1007/s00202-017-0654-8

Gogna, A., and Tayal, A. (2013). Metaheuristics: review and application. *J. Exp. Theor. Artif. Intell.* 25, 503–526. doi:10.1080/0952813x.2013.782347

Heidari, A. A., Abbaspour, R. A., and Jordehi, A. R. (2017). An efficient chaotic water cycle algorithm for optimization tasks. *Neural comput. Appl.* 28, 57–85. doi:10.1007/s00521-015-2037-2

Heidari, A. A., Mirjalili, S., Faris, H., Aljarah, I., Mafarja, M., Chen, H., et al. (2019). Harris hawks optimization: algorithm and applications. *Future Gener. Comput. Syst.* 97, 849–872. doi:10.1016/j.future.2019.02.028

Huang, C., Wang, L., Yeung, R. S.-C., Zhang, Z., Chung, H. S.-H., Bensoussan, A., et al. (2017a). A prediction model-guided jaya algorithm for the pv system maximum power point tracking. *IEEE Trans. Sustain. Energy* 9, 45–55. doi:10.1109/tste.2017.2714705

Huang, C., Zhang, Z., Wang, L., Song, Z., and Long, H. (2017b). "A novel global maximum power point tracking method for pv system using jaya algorithm," in 2017 IEEE Conference on Energy Internet and Energy System Integration (EI2), Beijing, China, November 26–28, 2017 (IEEE), 1–5.

Jadon, S. S., Tiwari, R., Sharma, H., and Bansal, J. C. (2017). Hybrid artificial bee colony algorithm with differential evolution. *Appl. Soft Comput.* 58, 11–24. doi:10.1016/j.asoc.2017.04.018

Kabir, E., Kumar, P., Kumar, S., Adelodun, A. A., and Kim, K.-H. (2018). Solar energy: potential and future prospects. *Renew. Sustain. Energy Rev.* 82, 894–900. doi:10.1016/j.rser.2017.09.094

Karaboga, D., and Akay, B. (2009). A comparative study of artificial bee colony algorithm. *Appl. Math. Comput.* 214, 108–132. doi:10.1016/j.amc.2009.03.090

Kavya, M., and Jayalalitha, S. (2021). Developments in perturb and observe algorithm for maximum power point tracking in photo voltaic panel: a review. *Arch. Comput. Methods Eng.* 28, 2447–2457. doi:10.1007/s11831-020-09461-x

Khare, A., and Rangnekar, S. (2013). A review of particle swarm optimization and its applications in solar photovoltaic system. *Appl. Soft Comput.* 13, 2997–3006. doi:10.1016/j.asoc.2012.11.033

Kjær, S. B. (2012). Evaluation of the "hill climbing" and the "incremental conductance" maximum power point trackers for photovoltaic power systems. *IEEE Trans. Energy Convers.* 27, 922–929. doi:10.1109/TEC.2012.2218816

Koad, R. B., Zobaa, A. F., and El-Shahat, A. (2016). A novel mppt algorithm based on particle swarm optimization for photovoltaic systems. *IEEE Trans. Sustain. Energy* 8, 468–476. doi:10.1109/tste.2016.2606421

Li, G., Jin, Y., Akram, M., Chen, X., and Ji, J. (2018). Application of bio-inspired algorithms in maximum power point tracking for pv systems under partial shading conditions–a review. *Renew. Sustain. Energy Rev.* 81, 840–873. doi:10.1016/j.rser.2017.08.034

Li, H., Yang, D., Su, W., Lü, J., and Yu, X. (2018). An overall distribution particle swarm optimization mppt algorithm for photovoltaic system under partial shading. *IEEE Trans. Ind. Electron.* 66, 265–275. doi:10.1109/tie.2018.2829668

Li, X., Zhu, Y., Wen, H., Du, Y., and Xiao, W. (2022). Reference-voltage-line-aided power incremental algorithm for photovoltaic gmppt and partial shading detection. *IEEE Trans. Sustain. Energy* 13, 1756–1770. doi:10.1109/tste.2022.3174614

Lian, K., Jhang, J., and Tian, I. (2014). A maximum power point tracking method based on perturb-and-observe combined with particle swarm optimization. *IEEE J. Photovolt.* 4, 626–633. doi:10.1109/jphotov.2013.2297513

Lones, M. A. (2014). "Metaheuristics in nature-inspired algorithms," in Proceedings of the Companion Publication of the 2014 Annual Conference on Genetic and Evolutionary Computation, Vancouver, Canada, July, 2014. 1419–1422.

Ma, J., Hong, D., Wang, K., Bi, Z., Zhu, X., Zhang, J., et al. (2022). Analytical modeling and parameter estimation of photovoltaic strings under partial shading conditions. *Sol. Energy Mater. Sol. Cells* 235, 111494. doi:10.1016/j.solmat.2021.111494

Mamarelis, E., Petrone, G., and Spagnuolo, G. (2014). A two-steps algorithm improving the p&o steady state mppt efficiency. *Appl. Energy* 113, 414–421. doi:10.1016/j.apenergy.2013.07.022

Mansoor, M., Mirza, A. F., and Ling, Q. (2020). Harris hawk optimization-based mppt control for pv systems under partial shading conditions. *J. Clean. Prod.* 274, 122857. doi:10.1016/j.jclepro.2020.122857

Mao, M., Cui, L., Zhang, Q., Guo, K., Zhou, L., Huang, H., et al. (2020). Classification and summarization of solar photovoltaic mppt techniques: a review based on traditional and intelligent control strategies. *Energy Rep.* 6, 1312–1327. doi:10.1016/j.egyr.2020.05.013

Mao, M., Zhang, L., Duan, P., Duan, Q., and Yang, M. (2018). Grid-connected modular pv-converter system with shuffled frog leaping algorithm based dmppt controller. *Energy* 143, 181–190. doi:10.1016/j.energy.2017.10.099

Mareli, M., and Twala, B. (2018). An adaptive cuckoo search algorithm for optimisation. *Appl. Comput. Inf.* 14, 107–115. doi:10.1016/j.aci.2017.09.001

Mirza, A. F., Mansoor, M., Zhan, K., and Ling, Q. (2021). High-efficiency swarm intelligent maximum power point tracking control techniques for varying temperature and irradiance. *Energy* 228, 120602. doi:10.1016/j.energy.2021.120602

Moosavi, S. H. S., and Bardsiri, V. K. (2017). Satin bowerbird optimizer: a new optimization algorithm to optimize anfis for software development effort estimation. *Eng. Appl. Artif. Intell.* 60, 1–15. doi:10.1016/j.engappai.2017.01.006

Mosaad, M. I., abed el Raouf, M. O., Al-Ahmar, M. A., and Banakher, F. A. (2019). Maximum power point tracking of pv system based cuckoo search algorithm; review and comparison. *Energy Procedia* 162, 117–126. doi:10.1016/j.egypro.2019.04.013

Motahhir, S., El Hammoumi, A., and El Ghzizal, A. (2020). The most used mppt algorithms: review and the suitable low-cost embedded board for each algorithm. *J. Clean. Prod.* 246, 118983. doi:10.1016/j.jclepro.2019.118983

Nakrani, S., and Tovey, C. (2004). On honey bees and dynamic server allocation in internet hosting centers. *Adapt. Behav.* 12, 223–240. doi:10.1177/105971230401200308

Neri, F., and Cotta, C. (2012). Memetic algorithms and memetic computing optimization: a literature review. *Swarm Evol. Comput.* 2, 1–14. doi:10.1016/j.swevo.2011.11.003

Özkış, A., and Babalık, A. (2017). A novel metaheuristic for multi-objective optimization problems: the multi-objective vortex search algorithm. *Inf. Sci.* 402, 124–148. doi:10.1016/j.ins.2017.03.026

Padmanaban, S., Priyadarshi, N., Bhaskar, M. S., Holm-Nielsen, J. B., Hossain, E., Azam, F., et al. (2019). A hybrid photovoltaic-fuel cell for grid integration with jaya-based maximum power point tracking: experimental performance evaluation. *IEEE Access* 7, 82978–82990. doi:10.1109/access.2019.2924264

Patel, H., and Agarwal, V. (2008). Maximum power point tracking scheme for pv systems operating under partially shaded conditions. *IEEE Trans. Ind. Electron.* 55, 1689–1698. doi:10.1109/tie.2008.917118

Pavlyukevich, I. (2007). Lévy flights, non-local search and simulated annealing. *J. Comput. Phys.* 226, 1830–1844. doi:10.1016/j.jcp.2007.06.008

Pilakkat, D., and Kanthalakshmi, S. (2019). An improved p&o algorithm integrated with artificial bee colony for photovoltaic systems under partial shading conditions. *Sol. Energy* 178, 37–47. doi:10.1016/j.solener.2018.12.008

Pilakkat, D., and Kanthalakshmi, S. (2020). Single phase pv system operating under partially shaded conditions with abc-po as mppt algorithm for grid connected applications. *Energy Rep.* 6, 1910–1921. doi:10.1016/j.egyr.2020.07.019

Ram, J. P., Manghani, H., Pillai, D. S., Babu, T. S., Miyatake, M., Rajasekar, N., et al. (2018). Analysis on solar pv emulators: a review. *Renew. Sustain. Energy Rev.* 81, 149–160. doi:10.1016/j.rser.2017.07.039

Rao, R. (2016). Jaya: a simple and new optimization algorithm for solving constrained and unconstrained optimization problems. *Int. J. Industrial Eng. Comput.* 7, 19–34. doi:10.5267/j.ijiec.2015.8.004

Rao, R. V., and Saroj, A. (2017). A self-adaptive multi-population based jaya algorithm for engineering optimization. *Swarm Evol. Comput.* 37, 1–26. doi:10.1016/j.swevo.2017.04.008

Rao, R. V., Savsani, V. J., and Vakharia, D. (2012). Teaching–learning-based optimization: an optimization method for continuous non-linear large scale problems. *Inf. Sci.* 183, 1–15. doi:10.1016/j.ins.2011.08.006

Reisi, A. R., Moradi, M. H., and Jamasb, S. (2013). Classification and comparison of maximum power point tracking techniques for photovoltaic system: a review. *Renew. Sustain. energy Rev.* 19, 433–443. doi:10.1016/j.rser.2012.11.052

Rezk, H., Fathy, A., and Abdelaziz, A. Y. (2017). A comparison of different global mppt techniques based on meta-heuristic algorithms for photovoltaic system subjected to partial shading conditions. *Renew. Sustain. Energy Rev.* 74, 377–386. doi:10.1016/j.rser.2017.02.051

Rezk, H., and Fathy, A. (2017). Simulation of global mppt based on teaching–learning-based optimization technique for partially shaded pv system. *Electr. Eng.* 99, 847–859. doi:10.1007/s00202-016-0449-3

Samy, M., Barakat, S., and Ramadan, H. (2019). A flower pollination optimization algorithm for an off-grid pv-fuel cell hybrid renewable system. *Int. J. hydrogen energy* 44, 2141–2152. doi:10.1016/j.ijhydene.2018.05.127

Sarvi, M., Soltani, I., and Avanaki, I. (2014). A water cycle algorithm maximum power point tracker for photovoltaic energy conversion system under partial shading condition. *Appl. Math. Eng. Manag. Technol.* 2, 103–116.

Seyedmahmoudian, M., Horan, B., Soon, T. K., Rahmani, R., Oo, A. M. T., Mekhilef, S., et al. (2016). State of the art artificial intelligence-based mppt techniques for mitigating partial shading effects on pv systems–a review. *Renew. Sustain. Energy Rev.* 64, 435–455. doi:10.1016/j.rser.2016.06.053

Shams, I., Mekhilef, S., and Tey, K. S. (2020). Maximum power point tracking using modified butterfly optimization algorithm for partial shading, uniform shading, and fast varying load conditions. *IEEE Trans. Power Electron.* 36, 5569–5581. doi:10.1109/tpel.2020.3029607

Shi, J., Zhang, W., Zhang, Y., Xue, F., and Yang, T. (2015). Mppt for pv systems based on a dormant pso algorithm. *Electr. Power Syst. Res.* 123, 100–107. doi:10.1016/j.epsr.2015.02.001

Soufi, Y., Bechouat, M., and Kahla, S. (2017). Fuzzy-pso controller design for maximum power point tracking in photovoltaic system. *Int. J. hydrogen energy* 42, 8680–8688. doi:10.1016/j.ijhydene.2016.07.212

Soufyane Benyoucef, A., Chouder, A., Kara, K., Silvestre, S., and sahed, O. A. (2015). Artificial bee colony based algorithm for maximum power point tracking (mppt) for pv systems operating under partial shaded conditions. *Appl. Soft Comput.* 32, 38–48. doi:10.1016/j.asoc.2015.03.047

Sridhar, R., Jeevananthan, S., Dash, S. S., and Vishnuram, P. (2017). A new maximum power tracking in pv system during partially shaded conditions based on shuffled frog leap algorithm. *J. Exp. Theor. Artif. Intell.* 29, 481–493. doi:10.1080/0952813x.2016.1186750

Sundararaj, V., Anoop, V., Dixit, P., Arjaria, A., Chourasia, U., Bhambri, P., et al. (2020). Ccgpa-mppt: cauchy preferential crossover-based global pollination algorithm for mppt in photovoltaic system. *Prog. Photovolt. Res. Appl.* 28, 1128–1145. doi:10.1002/pip.3315

Sundareswaran, K., Sankar, P., Nayak, P. S. R., Simon, S. P., and Palani, S. (2015a). Enhanced energy output from a pv system under partial shaded conditions through artificial bee colony. *IEEE Trans. Sustain. Energy* 6, 198–209. doi:10.1109/tste.2014.2363521

Sundareswaran, K., Vigneshkumar, V., Sankar, P., Simon, S. P., Nayak, P. S. R., Palani, S., et al. (2015b). Development of an improved p&o algorithm assisted through a colony of foraging ants for mppt in pv system. *IEEE Trans. Ind. Inf.* 12, 187–200. doi:10.1109/tii.2015.2502428

Teshome, D., Lee, C., Lin, Y., and Lian, K. (2016). A modified firefly algorithm for photovoltaic maximum power point tracking control under partial shading. *IEEE J. Emerg. Sel. Top. Power Electron.* 5, 661–671. doi:10.1109/jestpe.2016.2581858

Tey, K. S., and Mekhilef, S. (2014). Modified incremental conductance algorithm for photovoltaic system under partial shading conditions and load variation. *IEEE Trans. Ind. Electron.* 61, 5384–5392. doi:10.1109/tie.2014.2304921

Wang, C., and Liu, K. (2019). A randomly guided firefly algorithm based on elitist strategy and its applications. *IEEE Access* 7, 130373–130387. doi:10.1109/access.2019.2940582

Wang, G.-G., Deb, S., and Cui, Z. (2019). Monarch butterfly optimization. *Neural comput. Appl.* 31, 1995–2014. doi:10.1007/s00521-015-1923-y

Xiao, W., Dunford, W. G., Palmer, P. R., and Capel, A. (2007). Application of centered differentiation and steepest descent to maximum power point tracking. *IEEE Trans. Ind. Electron.* 54, 2539–2549. doi:10.1109/tie.2007.899922

Xiao, W., El Moursi, M. S., Khan, O., and Infield, D. (2016). Review of grid-tied converter topologies used in photovoltaic systems. *IET Renew. Power Gener.* 10, 1543–1551. doi:10.1049/iet-rpg.2015.0521

Xue, J., and Shen, B. (2020). A novel swarm intelligence optimization approach: sparrow search algorithm. *Syst. Sci. Control Eng.* 8, 22–34. doi:10.1080/21642583.2019.1708830

Yang, B., Wang, J., Zhang, X., Yu, T., Yao, W., Shu, H., et al. (2020). Comprehensive overview of meta-heuristic algorithm applications on pv cell parameter identification. *Energy Convers. Manag.* 208, 112595. doi:10.1016/j.enconman.2020.112595

Yang, X.-S., and Deb, S. (2009). "Cuckoo search via lévy flights," in 2009 World Congress on Nature & Biologically Inspired Computing (NaBIC), Coimbatore, India, December 9–11, 2009 (IEEE), 210–214.

Yang, X.-S., and Deb, S. (2013). Multiobjective cuckoo search for design optimization. *Comput. Operations Res.* 40, 1616–1624. doi:10.1016/j.cor.2011.09.026

Yang, X.-S. (2009). "Firefly algorithms for multimodal optimization," in International Symposium on Stochastic Algorithms, Sapporo, Japan, October 26–28, 2009 (Springer), 169–178.

Yang, X.-S. (2012). "Flower pollination algorithm for global optimization," in International Conference on Unconventional Computing and Natural Computation, Orléans, France, September 3–7, 2012 (Springer), 240–249.

Yao, K., and Gao, J. (2015). Law of large numbers for uncertain random variables. *IEEE Trans. Fuzzy Syst.* 24, 615–621. doi:10.1109/tfuzz.2015.2466080

Yilmaz, S., and Sen, S. (2019). Electric fish optimization: a new heuristic algorithm inspired by electrolocation. *Neural comput. Appl.* 32, 11543–11578. doi:10.1007/s00521-019-04641-8

Yousri, D., Babu, T. S., Allam, D., Ramachandaramurthy, V. K., and Etiba, M. B. (2019). A novel chaotic flower pollination algorithm for global maximum power point tracking for photovoltaic system under partial shading conditions. *IEEE Access* 7, 121432–121445. doi:10.1109/access.2019.2937600

Zaldivar, D., Morales, B., Rodríguez, A., Valdivia-G, , A., Cuevas, E., Pérez-Cisneros, M., et al. (2018). A novel bio-inspired optimization model based on yellow saddle goatfish behavior. *Biosystems* 174, 1–21. doi:10.1016/j.biosystems.2018.09.007

Zhao, W., Wang, L., and Zhang, Z. (2019). Artificial ecosystem-based optimization: a novel nature-inspired meta-heuristic algorithm. *Neural comput. Appl.* 32, 9383–9425. doi:10.1007/s00521-019-04452-x

Zhou, C., Huang, L., Ling, Z., and Cui, Y. (2021). Research on mppt control strategy of photovoltaic cells under multi-peak. *Energy Rep.* 7, 283–292. doi:10.1016/j.egyr.2021.01.068

Nomenclature

V_{set}	voltage set-point

V_{oc}	open-circuit voltage

I_{sc}	short-circuit current

L	Lévy flight

T_{max}	maximum number of iterations

I_{pv}	photo-generated current

I_s	reverse saturation current of the diode

N_s	number of PV cells connected in series

N_m	number of PV modules connected in series

q	electron charge constant

k	Boltzmann constant

R_s	series resistance

R_p	shunt resistance

T	temperature of the PN junction in Kelvin

k	Boltzmann constant

$I_{sat, bp}$	reverse bias saturation current of the bypass diode

v_i^t	The ith particle's speed

n_1, n_2	learning constants

p_i	individual best of ith particle

p_g	global best of particles

P_w	The worst frog

P_b	The best frog

$\mathcal{F}$	power value

β	attractiveness

I	brightness

r_{ij}	The Euclidean distance between the i and j fireflies

TF	Teacher factor

V_s	terminal voltage of a PV string

P_{est}	The estimated power value

P_{GMPP}	The global maximum power value

N_{best}	The iteration index when the output power reaches 95% P_{est}

$\mathcal{R}_{0, 1}$	Random number within [0, 1]

$\mathcal{R}_{-1, 1}$	Random number within [−1, 1]

$\mathcal{R}_{-0.5, 0.5}$	Random number within [−0.5, 0.5]

t	The iteration index